

# Theranostics in Nuclear Medicine: Emerging and Re-emerging Integrated Imaging and Therapies in the Era of Precision Oncology

José Flávio Gomes Marin, MD

Rafael F Nunes, MD

Artur M. Coutinho, MD, PhD

Elaine C. Zaniboni, MD

Larissa B. Costa, MD

Felipe G. Barbosa, MD

Marcelo A. Queiroz, MD

Giovanni G. Cerri, MD, PhD

Carlos A. Buchpiguel, MD, PhD

**Abbreviations:** DOTATATE = tetraazacyclododecane tetraacetic acid-octreotate, EDTMP = ethylenediaminetetramethylene phosphonic acid, FDG =  $^{18}\text{F}$ -fluorodeoxyglucose, HEDP = hydroxyethylidene diphosphonic acid, HER2 = human epidermal growth factor receptor 2, MAA = macroaggregates of human serum albumin, mCRPC = castration-resistant metastatic prostate cancer, MIBG = metaiodobenzylguanidine, MIP = maximum intensity projection, PRLT = PSMA-targeted radioligand therapy, PRRT = peptide receptor radionuclide therapy, PSMA = prostate-specific membrane antigen, SSTR = somatostatin receptor, WBS = whole-body scintigraphy

**RadioGraphics** 2020; 40:1715–1740

<https://doi.org/10.1148/rg.2020200021>

**Content Codes:** **MI** **NM** **OI**

From the Department of Radiology, Hospital Sírio-Libanês, Rua Dona Adma Jafet 115, CEP 01308-060, São Paulo, SP, Brazil (J.F.G.M., R.F.N., A.M.C., E.C.Z., L.B.C., F.G.B., M.A.Q., G.G.C., C.A.B.); and Department of Radiology and Oncology, Hospital das Clínicas HCF-MUSP, Faculdade de Medicina, Universidade de São Paulo, São Paulo, SP, Brazil (J.F.G.M., A.M.C., M.A.Q., G.G.C., C.A.B.). Recipient of a Magna Cum Laude award for an education exhibit at the 2019 RSNA Annual Meeting. Received March 16, 2020; revision requested April 23 and received May 23; accepted June 12. For this journal-based SA-CME activity, the authors, editor, and reviewers have disclosed no relevant relationships. **Address correspondence to** J.F.G.M. (e-mail: [jfgmarin@yahoo.com.br](mailto:jfgmarin@yahoo.com.br)).

See discussion on this article by Greenspan and Jadvar (pp 1741–1742).

©RSNA, 2020

Theranostics refers to the pairing of diagnostic biomarkers with therapeutic agents that share a specific target in diseased cells or tissues. Nuclear medicine, particularly with regard to applications in oncology, is currently one of the greatest components of the theranostic concept in clinical and research scenarios. Theranostics in nuclear medicine, or nuclear theranostics, refers to the use of radioactive compounds to image biologic phenomena by means of expression of specific disease targets such as cell surface receptors or membrane transporters, and then to use specifically designed agents to deliver ionizing radiation to the tissues that express these targets. The nuclear theranostic approach has sparked increasing interest and gained importance in parallel to the growth in molecular imaging and personalized medicine, helping to provide customized management for various diseases; improving patient selection, prediction of response and toxicity, and determination of prognosis; and avoiding futile and costly diagnostic examinations and treatment of many diseases. The authors provide an overview of theranostic approaches in nuclear medicine, starting with a review of the main concepts and unique features of nuclear theranostics and aided by a retrospective discussion of the progress of theranostic agents since early applications, with illustrative cases emphasizing the imaging features. Advanced concepts regarding the role of fluorine 18-fluorodeoxyglucose PET in theranostics, as well as developments in and future directions of theranostics, are discussed.

©RSNA, 2020 • [radiographics.rsna.org](https://radiographics.rsna.org)

## SA-CME LEARNING OBJECTIVES

*After completing this journal-based SA-CME activity, participants will be able to:*

- Describe the concept and potential advantages of the theranostic approach in nuclear medicine.
- List and discuss the main theranostic procedures (classic and modern) in nuclear medicine.
- Discuss less frequently addressed issues regarding the nuclear theranostic approach, such as the pivotal role of FDG PET and the limitations of the theranostic model.

*See [rsna.org/learning-center-rg](https://rsna.org/learning-center-rg).*

## Introduction

In 1900, German researcher and Nobel Prize laureate Paul Ehrlich proposed the “magic bullet” concept (1). Magic bullets were idealized as special drugs with chemical and biologic properties that would enable the agents to precisely find and kill disease foci with no damage to healthy tissues. Ehrlich’s works and theories regarding new dyes, histologic findings, and immunology fields revolutionized the

## TEACHING POINTS

- Theranostics is essentially the coupling of diagnostic and therapeutic tools related to the same specific molecular targets, enabling more accurate patient selection, prediction of treatment response and tissue toxicity, and response evaluation, with the goal of better outcomes.
- Diagnostic and therapeutic radiopharmaceuticals that access the same cellular structure and biologic process—that is, that share the same target—are called theranostic pairs.
- Most of the theranostic procedures discussed earlier in this article are directed against specific cell phenotypes that generally require a degree of differentiation sufficient to be satisfactorily expressed and consequently targeted.
- FDG PET has a pivotal role in the theranostic approach, enabling better patient selection through characterization of more undifferentiated and/or aggressive phenotypes and avoiding ineffective, potentially toxic, and costly treatments.
- The specificity of the therapeutic component of theranostic pairs is not perfect, as it is impossible to deliver radiation to only the target lesions and avoid compromising adjacent non-target tissues.

comprehension, discovery, and design of drugs, serving as the basis of modern chemotherapy and targeted therapies in medicine (2). More than 100 years after being proposed, the magic bullet concept remains current and influences the search and development of specific effective and harmless molecule-driven treatments for human diseases, most notably cancer. Recently, terms such as *personalized medicine*, *targeted medicine*, and *precision medicine* have been used to represent this idea.

As a central component of patient care, imaging has followed, and often made possible, discoveries of drugs and treatments, evolving from a valuable diagnostic tool to a now powerful guide for enhancing disease characterization, patient selection, prediction of treatment response and tissue toxicity, and determination of the prognosis (3,4). In summary, imaging is integrated into therapy now more than ever before. In this context, an approach referred to as theranostics has been frequently used. *Theranostics* is a hybrid term that refers to the fusion of two words, *therapy* and *diagnostics*, and this approach was first proposed in 2002 (5). Although the term is reportedly new, the concept behind theranostics is not and has been applied and revisited over the years (6). Theranostics is essentially the coupling of diagnostic and therapeutic tools related to the same specific molecular targets, enabling more accurate patient selection, prediction of treatment response and tissue toxicity, and response evaluation, with the goal of better outcomes.

In essence, theranostics refers to any combination of diagnostic and therapeutic modalities, for any disease. For example, immunohistochemical staining for human epidermal growth factor recep-

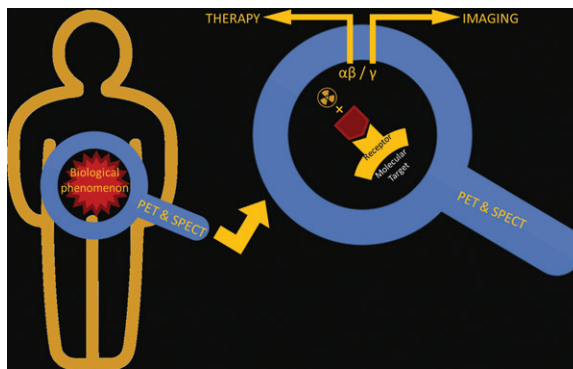


**Figure 1.** Diagram provides an introductory overview of nuclear theranostics. Specific agents may be labeled with a  $\gamma$ -emitting radionuclide for PET/SPECT imaging, in combination with an  $\alpha$ - or  $\beta$ -particle-emitting radionuclide (suitable for therapy).

tor 2 (HER2) receptors in a breast cancer specimen to select patients who are suitable for specific treatment with anti-HER2 receptor antibodies (eg, trastuzumab) is a well-established theranostic approach (7). However, in the literature, the term *theranostics* has been more frequently associated with some *in vivo* nuclear medicine oncologic applications; this scenario exemplifies the modern concept of theranostics and is the main focus of discussion in this article. Therefore, throughout this article, *theranostics* will be used in reference to nuclear medicine theranostics specifically.

## Contextualization of Nuclear Theranostics

Nuclear medicine imaging is mainly based on the principle of using radioactive isotopes linked to specific molecules (ie, radiopharmaceutical agents or radiotracers) to assess key biologic pathways, especially the pathophysiologic features of diseases (8). Therapy in nuclear medicine acts in the same way: Radiopharmaceutical agents are used to target diseased tissue, with radiation applied at the cellular level by way of a specific chemical and/or biologic affinity. The imaging or therapeutic capability of each radioisotope is determined according to the type of radiation emitted because electromagnetic radiation (ie,  $\gamma$  rays) can be detected by imaging systems (scintigraphy, SPECT, and PET), and particulate irradiations have cytotoxic (ie, therapeutic) properties (Fig 1).

There are two main forms of particulate radiation used for therapeutic applications: radiation with  $\alpha$  particles and radiation with  $\beta$  particles (which are electrons). These two forms of radiation share a common feature: a high transfer of energy to tissues that leads to severe cellular injury due to DNA damage. The  $\alpha$  particles have higher energy and much greater mass. Some isotopes (eg, lutetium 177 [ $^{177}\text{Lu}$ ]) can emit both electromag-

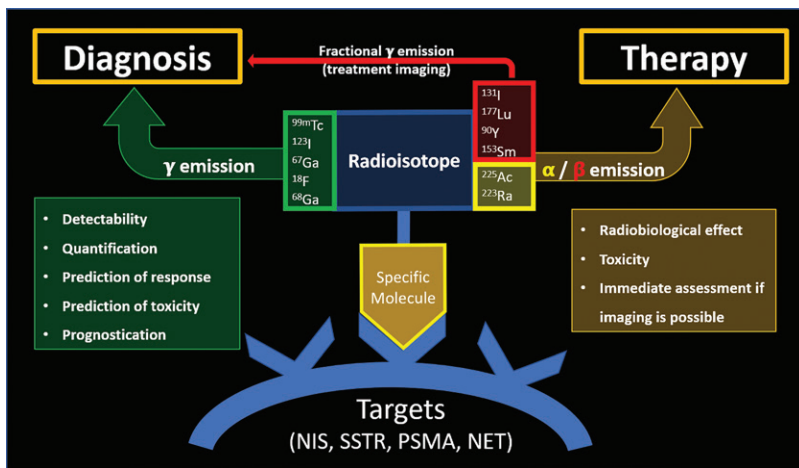


**Figure 2.** Diagram summarizes the theranostic approach in nuclear medicine, including the diagnostic and therapeutic components and their respective radioisotopes and advantages. Examples of frequent targets are illustrated. <sup>225</sup>Ac = actinium 225, <sup>18</sup>F = fluorine 18, <sup>67</sup>Ga = gallium 67, <sup>68</sup>Ga = gallium 68, <sup>123</sup>I = iodine 123, <sup>131</sup>I = iodine 131, NET = norepinephrine transporter, NIS = sodium iodide co-transporter, PSMA = prostate-specific membrane antigen, <sup>223</sup>Ra = radium 223, <sup>153</sup>Sm = samarium 153, SSTR = somatostatin receptor, <sup>99m</sup>Tc = technetium 99m, <sup>90</sup>Y = yttrium 90.

**Table 1: Theranostic Pairs Commonly Used in Clinical Nuclear Medicine Practice**

Diagnostic Agent(s)	Therapeutic Agent(s)	Target	Disease
<sup>123</sup> I (NaI)	<sup>131</sup> I (NaI)	NIS	Thyroid cancer, hyperthyroidism
<sup>123</sup> I-MIBG	<sup>131</sup> I-MIBG	NET	Neuroblastoma, pheochromocytoma-paraganglioma, MTC
<sup>99m</sup> Tc-medronate, <sup>18</sup> F-sodium fluoride	<sup>223</sup> Ra	Bone hydroxyapatite	Prostate cancer
<sup>68</sup> Ga-DOTA-based agents, * <sup>99m</sup> Tc-octreotide, <sup>111</sup> In-octreotide	<sup>177</sup> Lu-octreotate, <sup>90</sup> Y-octreotate	SSTR	Neuroendocrine tumors
<sup>68</sup> Ga-PSMA, <sup>18</sup> F-PSMA <sup>†</sup>	<sup>177</sup> Lu-PSMA, <sup>225</sup> Ac-PSMA <sup>†</sup>	PSMA	Prostate cancer
<sup>99m</sup> Tc-MAA	<sup>90</sup> Y microspheres	Hepatic microcirculation	HCC, cholangiocarcinoma, liver metastasis
Anti-CD20 IHC	<sup>131</sup> I-anti-CD20, <sup>90</sup> Y-anti-CD20	CD20	Non-Hodgkin lymphoma

Note.—CD20 = B-lymphocyte antigen CD20, DOTA = tetraazacyclododecane tetraacetic acid, HCC = hepatocellular carcinoma, IHC = immunohistochemistry, <sup>111</sup>In = indium 111, MAA = macroaggregates of human serum albumin, MIBG = metaiodobenzylguanidine, MTC = medullary thyroid carcinoma, NaI = sodium iodide, NET = norepinephrine transporter, NIS = sodium iodide co-transporter.

\*<sup>68</sup>Ga-DOTATATE (<sup>68</sup>Ga-tetraazacyclododecane tetraacetic acid-octreotide), <sup>68</sup>Ga-DOTATOC (<sup>68</sup>Ga-DOTA Phe1-Tyr<sup>3</sup>-octreotide), or <sup>68</sup>Ga-DOTANOC (<sup>68</sup>Ga-DOTA NaI<sup>3</sup>-octreotide).

<sup>†</sup>Use of these agents is not yet FDA approved.

netic and particulate radiation, making simultaneous treatment and imaging possible. Therefore, combining the emitting characteristics of different radioisotopes with specific molecules that target key cellular pathways is the mechanism of nuclear medicine theranostics (Fig 2). Diagnostic and therapeutic radiopharmaceuticals that access the same cellular structure and biologic process—that is, that share the same target—are called theranostic pairs (Table 1) (Fig 3). It is important to note that although most of the theranostic pairs currently used in nuclear medicine are formed from radiopharmaceuticals only, there are “hybrid” theranostic pairs formed from a radiopharmaceutical agent and a diagnostic or therapeutic component from other modalities, such as immunohistochemical staining and nonradioactive

targeted therapies such as antibody and tyrosine kinase inhibitor treatments (Table 2). Thus, different classes of “arrows” can be used for imaging or treatment of the same intended target.

Theranostics has been used in nuclear medicine for the past 8 decades. Radioiodine-based diagnosis, evaluation, and therapy for differentiated thyroid cancer was the first successful theranostic system and is the best example of a classic theranostic procedure that has maintained high clinical relevance in modern medicine (9). However, extensive developments in molecular biology, radiochemistry, and imaging technology in the past 2 decades, in particular the emergence of hybrid imaging examinations such as SPECT/CT, PET/CT, and PET/MRI, have led to the availability of cutting-edge theranostic procedures



**Figure 3.** Whole-body pre- and posttreatment images show the use of theranostic pairs in nuclear medicine in the same patient. *A*, Anterior (left) and posterior (right)  $^{111}\text{In}$ -octreotide planar diagnostic scintigrams. *B*, Anterior maximum intensity projection (MIP)  $^{68}\text{Ga}$ -DOTATATE PET scan before treatment. *C*, Anterior (left) and posterior (right) fractional  $\gamma$ -ray  $^{177}\text{Lu}$ -octreotate planar scintigrams immediately after treatment. Note the better image quality and lesion conspicuity at pretreatment  $^{68}\text{Ga}$ -DOTATATE PET compared with those at  $^{111}\text{In}$ -octreotide scintigraphy. *WBS* = whole-body scintigraphy.

**Table 2: Theranostic Pairs Currently Being Evaluated**

Diagnostic Component	Therapeutic Component	Molecular Target	Disease
$^{68}\text{Ga}$ -CXCR4	$^{177}\text{Lu}$ -CXCR4	CXCR4	Multiple myeloma
$^{89}\text{Zr}$ , $^{18}\text{F}$ -anti-PD, PD-L1	Anti-PD-1, PD-L1	PD-1, PD-L1	Various tumors
$^{89}\text{Zr}$ -anti-HER2	Anti-HER2	HER2	Breast cancer

Note.—CXCR4 = chemokine receptor type 4, PD = programmed cell death protein, PD-L1 = programmed death-ligand 1,  $^{89}\text{Zr}$  = zirconium 89.

(some with a high level of evidence) and improved the quality of classic procedures.

### Classic Theranostic Agents

As mentioned earlier, systematic investigation of theranostic agents in nuclear medicine started with procedures involving the use of radioiodine and dates back to 1936 when Dr Saul Hertz had the idea that radioactive isotopes of iodine could be used to evaluate iodine metabolism (documented by James Means, MD, chair of medicine, Massachusetts General Hospital [MGH]) (10). Animal studies of thyroid metabolism began in 1937 and 1938, with  $^{131}\text{I}$  synthesized in the cyclotron at the University of California, Berkeley. Dr Hertz and Dr Arthur Roberts began treating patients with hyperthyroidism by using radioactive iodine at Massachusetts General Hospital in 1941. The radioactive iodine was produced in the cyclotron at the Massachusetts Institute of Technology. Hertz and Roberts performed seminal studies on the clinical use of radioiodine (11). Because of its use in a relevant clinical scenario—thyroid disease treatment— $^{131}\text{I}$  became important in clinical practice. Thus, the beginning of theranostics was simultaneous with the beginning of nuclear medicine itself as a relevant clinical specialty.

Other radioisotopes have since been incorporated into clinical practice. However, most of these agents were not evaluated within the context of evidence-based medicine, and thus far, there have been few or no phase 3 or randomized clinical trials to evaluate their effects, as compared with the effects of other treatments. In some cases, such as the use of radioiodine for differentiated thyroid cancer treatment, these agents have had no competition and are currently the primary treatment option (11–13).

### Radioiodine for Differentiated Thyroid Cancer

**Rationale and Clinical Aspects.**—Radioisotopes of sodium iodide,  $^{131}\text{I}$  in particular, classically have been used to diagnose and treat differentiated thyroid cancer (Fig 4) (11,14). Iodide, an essential component used to produce thyroid hormone, is captured by thyroid follicular cells and differentiated neoplastic thyroid cells mainly through the NaI membrane symporter, making it a cellular target for differentiated thyroid cancer. This target can be shared by other iodine isotopes and other diagnostic radiopharmaceuticals (eg,  $^{99\text{m}}\text{Tc}$ -pertechnetate) that can “pair” with

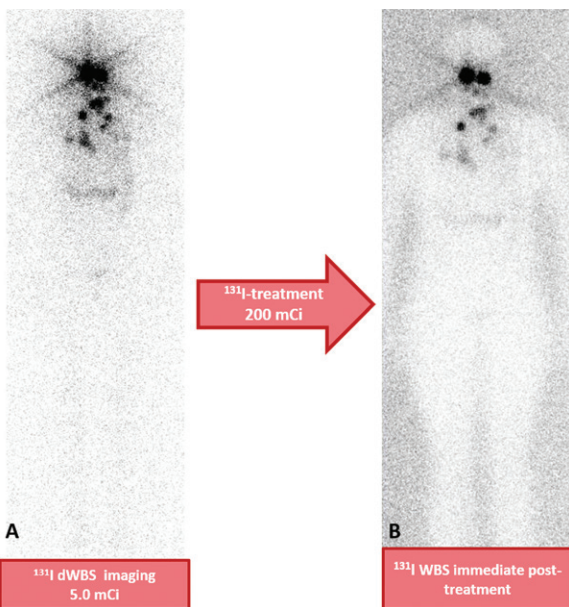


**Figure 4.** Pulmonary and mediastinal metastases depicted at  $^{131}\text{I}$  whole-body WBS, before, *A*, and after, *B*, treatment with  $^{131}\text{I}$  irradiation in a patient with thyroid cancer. *dWBS* = diagnostic WBS.

$^{131}\text{I}$ . The following iodine isotopes may be used as theranostic agents (12,14):

$^{131}\text{I}$  is a dual ( $\beta$ - and  $\gamma$ -ray) emitting isotope with a low cost and long half-life (~8 days) that is used for therapy and whole-body diagnostic scanning to identify remnant thyroid tissue or metastatic thyroid cancer. However, it is not an ideal diagnostic agent owing to its  $\gamma$ -ray emission pattern and long half-life, which result in poor image quality and a relatively high patient radiation dose.

$^{123}\text{I}$ , a purely  $\gamma$ -ray emitter, has a more optimal physical profile than  $^{131}\text{I}$  for diagnostic purposes in that it yields better image quality and involves a lower radiation burden. Thus, this isotope is also well suited for use in more recent approaches such as tomographic (SPECT) and hybrid imaging in conjunction with CT (SPECT/CT). For these reasons, despite its higher cost compared with  $^{131}\text{I}$ ,  $^{123}\text{I}$  is the most used iodine radioisotope for diagnostic scintigraphy in the United States.

Iodine 124 ( $^{124}\text{I}$ ), a promising diagnostic agent, is a positron emitter and is therefore used in PET. It is less frequently used clinically owing to its even higher production cost and lack of widespread availability.

In terms of therapeutic applications, radioiodine therapy with  $^{131}\text{I}$  remains the modality of choice for treating patients with differentiated thyroid cancer in the postoperative setting.  $^{131}\text{I}$  therapy can be performed by using different protocols for different purposes, taking into account factors such as initial extent of disease, surgical specimen characteristics, histologic subtype, imaging findings, and biochemical changes, which

ultimately determine the risk of disease recurrence. The applications for  $^{131}\text{I}$  therapy, which may be superimposed in the same patient, consist of ablation of residual normal tissue, adjuvant treatment of occult disease, and treatment of known local-regional or, especially, metastatic disease. Posttreatment images can be acquired in addition to pretreatment images, which, owing to the higher activity of  $^{131}\text{I}$  used in therapy, provide higher sensitivity in the assessment of metastatic lesions and overall staging, particularly in cases of small metastatic lesions such as micronodular lung metastases (15). The example case in Figure 5 illustrates the difference between pre- and post-treatment images (15–17).

### $^{131}\text{I}$ -MIBG for Neural Crest-derived Tumors

**Rationale and Clinical Aspects.**—The molecular analog of norepinephrine, MIBG labeled with  $^{131}\text{I}$  ( $^{131}\text{I}$ -MIBG), is another classic theranostic agent that is suitable for gamma camera and SPECT imaging, and it has been used in clinical settings since 1981.  $^{131}\text{I}$ -MIBG enters the neuroendocrine cells of the sympathetic nervous system by means of endocytosis or diffusion and remains stored in neurosecretory vesicles. It has high sensitivity (>90%) and specificity (>95%) for the detection of neural crest-derived (neuroectodermic) tumors and their secondary lesions (particularly in neuroblastoma, pheochromocytoma, and paraganglioma), complementing conventional imaging and indicating which tumors may benefit from radioisotopic therapy (12,18).

Like radioiodine,  $^{123}\text{I}$ -MIBG facilitates better imaging and is suitable for SPECT and SPECT/CT, but at a higher cost. Recent improvements in SPECT/CT techniques include the use of  $^{124}\text{I}$ -MIBG for PET, which yields higher spatial resolution and accuracy. Both  $^{123}\text{I}$ -MIBG and  $^{124}\text{I}$ -MIBG are limited to use for diagnostic purposes only, serving as imaging tracers, while  $^{131}\text{I}$ -MIBG is predominately used for therapeutics (19).

$^{123}\text{I}$ -MIBG imaging is the method of choice, particularly in pediatric patients, because of the lower radiation exposure with  $^{123}\text{I}$  and the risk of normal thyroid tissue damage from  $\beta$  particles when  $^{131}\text{I}$ -MIBG is used for imaging. Therefore, in patients exposed to  $^{131}\text{I}$ -MIBG, thyroidal uptake of free  $^{131}\text{I}$  should be blocked by saturating the gland with solutions containing nonradioactive iodine, such as potassium iodide, before the procedure (19).

MIBG-targeted theranostic indications include high-risk and either refractory or relapsed neuroblastoma, inoperable or metastatic pheochromocytoma, paraganglioma, carcinoid tumors, and

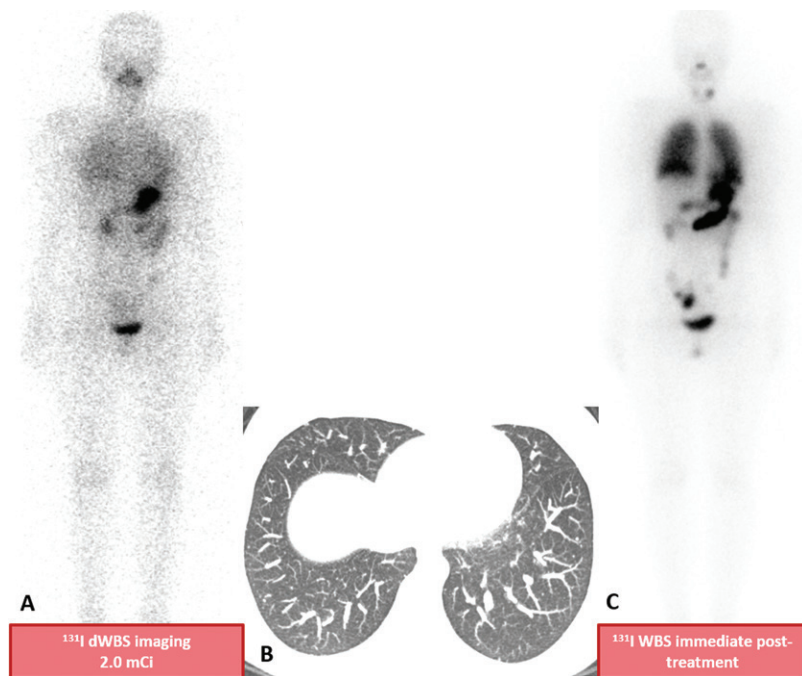
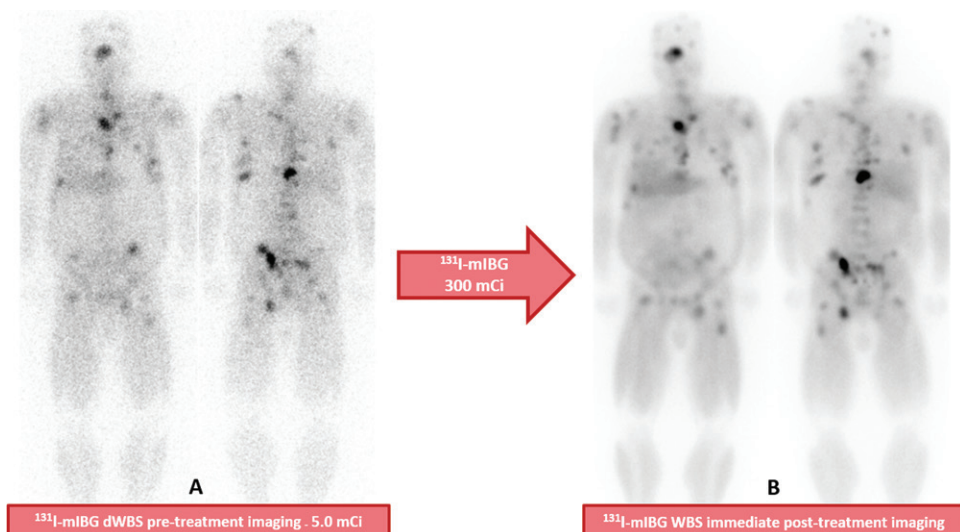


**Figure 5.** *A, C*, Pulmonary metastases depicted on anterior  $^{131}\text{I}$  WBS scans obtained before, *A*, and after, *C*, treatment in a patient with thyroid cancer. *B*, Only small micronodules are seen at axial thoracic CT. *dWBS* = diagnostic WBS.



metastatic or recurrent medullary thyroid carcinoma (Fig 6) (19,20). Recent data show promising results for the earlier use of MIBG in cases of neuroblastoma, as well as its combined use with  $^{177}\text{Lu}$ -DOTATATE, a more recently emerging theranostic approach.

**Neuroblastoma.**—Neuroblastomas are neural crest-derived tumors that exhibit highly variable clinical and pathologic behavior, and to date there is no consensus regarding the dose stratification by age (worst prognosis in children older than 18 months), tumor stage, or pathologic or molecular subtype. Most referred patients have high-risk (stage IV) disease at the time of therapy, leading to poor (<50%) disease-free survival at 5 years.

Treatment for most of these tumors includes surgery combined with radiation therapy for the primary tumor, which may not be possible at advanced stages of the disease, in association with chemotherapy and sometimes autologous stem-cell transplants and medication with drugs such as retinoic acid. However, most patients at high risk usually have a poor response to induction chemotherapy. There is significant uptake of MIBG in 90% of neuroblastoma cases (Fig 7). Treatment with  $^{131}\text{I}$ -MIBG classically has been restricted to use only in patients with refractory disease, but recent data suggest that it might be a suitable therapeutic agent for induction and consolidation in high-risk patients. Tumor response is around 68% during induction phases

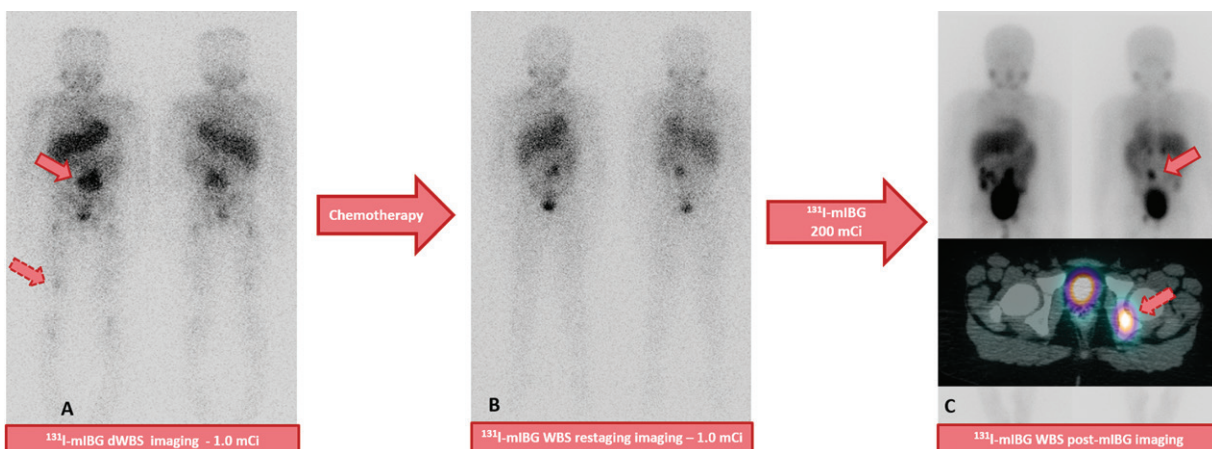


**Figure 7.** Classic theranostic approach, with anterior (left) and posterior (right)  $^{131}\text{I}$ -MIBG WBS scans used to diagnose, treat, and assess the treatment response of metastatic neuroblastoma in an 8-year-old patient. *A*, Diagnostic WBS (*dWBS*) scans show mesogastric (solid-outline arrow) and skeletal (dashed-outline arrow) lesions. *B*, Restaging WBS scans show a partial response after chemotherapy. *C*, Posttreatment therapeutic WBS scans (top) and axial SPECT/CT image (bottom) show delivery of the radiotracer to the mesogastric lesion (solid-outline arrow) and to a new bone lesion in the left acetabulum (dashed-outline arrow) that was not present at diagnostic imaging in *A*. Note: the higher sensitivity of posttherapeutic imaging is due to the use of a significantly higher dose of  $^{131}\text{I}$ -MIBG, causing the diagnostic and therapeutic features of this theranostic agent to overlap.

versus 32% in cases of recurrent or refractory tumors (20).

#### Pheochromocytoma and Paraganglioma.—

There are numerous retrospective studies and a few prospective studies investigating the use of  $^{131}\text{I}$ -MIBG for treatment of pheochromocytomas and paragangliomas, which are associated with relatively favorable outcomes.  $^{131}\text{I}$ -MIBG is mainly used as an adjunct to surgery, chemotherapy, and tyrosine kinase inhibitors in patients with metastasis. Usually, the therapy alleviates symptoms by lowering the level of circulating catecholamines. Rates of complete or partial treatment response are variable (~7%–62%) in different reports, mainly ranging from 25% to 30% of patients, and stable disease is seen in approximately 8% of patients. The radioactivity doses used also vary considerably among different studies, ranging from 100 to more than 2000 mCi (21,22).

Overall, there is a lack of randomized controlled trials in which  $^{131}\text{I}$ -MIBG treatment is compared with other treatments, different  $^{131}\text{I}$ -MIBG therapeutic regimens are compared, or different associations of  $^{131}\text{I}$ -MIBG and other therapies are compared. Most of the  $^{131}\text{I}$ -MIBG treatment schemes recently used are based on retrospective research, and only a few nonrandomized studies have been performed, with contradictory results that were mainly due to patient selection bias. There is also a lack of well-defined outcomes and treatment goals, such as the endpoints that should be considered valid (symptoms, tumor size, or survival measurements) and the thresholds that should be used to consider

disease progression, stability, or a partial versus complete treatment response.

#### Bone-seeking Therapeutic Radiopharmaceuticals

Agents used to reduce or alleviate pain include radiolabeled phosphonates such as rhenium 186- and rhenium 188-hydroxyethylidene diphosphonic acid (HEDP) and  $^{153}\text{Sm}$ -ethylenediaminetetraethylene phosphonic acid (EDTMP), which bind to metastatic bone lesions by means of an indirect mechanism of absorption to hydroxyapatite crystals, as well as calcium analogs such as strontium chloride 89. All of these agents are  $\beta$ -particle emitters. The bone matrix incorporates these radiopharmaceuticals owing to the increased osseous turnover induced by the metastatic lesions, a process best seen in osteoblastic lesions. Once incorporated by the bone matrix around the metastases, the isotopes emit  $\beta$  particles that induce cell death in the malignant lesions. Consequently, imaging of the theranostic process is usually performed with bone scintigraphy with use of phosphonates labeled with technetium, such as  $^{99\text{m}}\text{Tc}$ -medronate or  $^{99\text{m}}\text{Tc}$ -HEDP, which is administered before treatment to confirm the presence of and radiopharmaceutical uptake by lesions and thus increase the likelihood of treatment success (Fig 8) (12,13).

These pharmaceuticals serve as palliative treatments to relieve bone pain and improve quality of life; however, they have no proven effect on survival or in the disease course. Hence, they are now being replaced by  $^{223}\text{Ra}$ -dichloride, a short-range  $\alpha$ -particle-emitting calcium analog with a

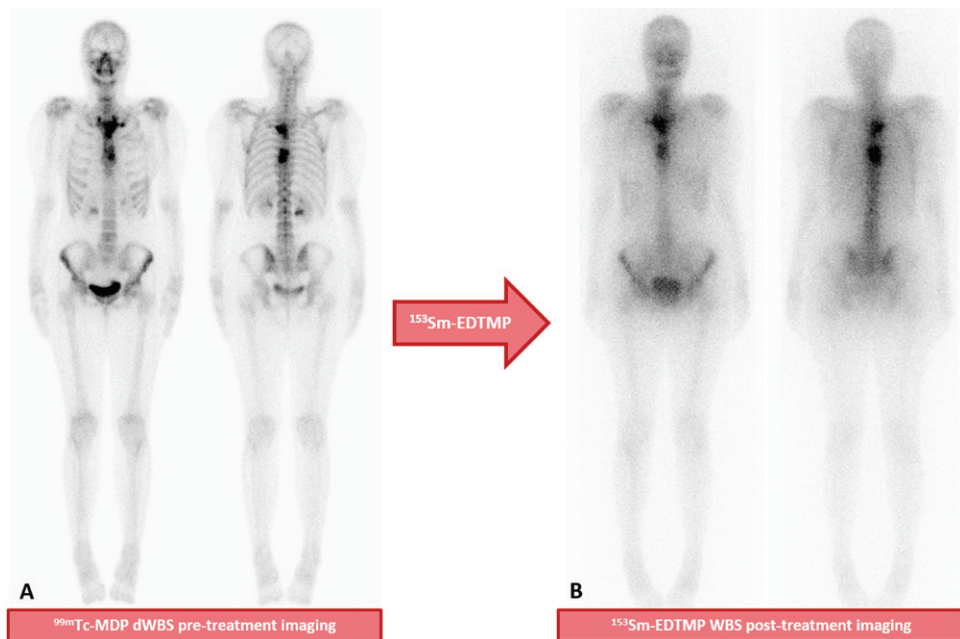


**Figure 8.** Bone-seeking theranostic agents used in a 53-year-old woman with metastatic breast cancer to the skeleton. *A*, Anterior (left) and posterior (right) diagnostic  $^{99m}\text{Tc}$ -medronate ( $^{99m}\text{Tc}$ -MDP) bone scans obtained before treatment show sternal and vertebral bone lesions with intense radiotracer uptake. *B*, Anterior (left) and posterior (right) scans obtained immediately after  $^{153}\text{Sm}$ -EDTMP administration, with  $\gamma$  fractional emission, show radiotracer uptake by bone lesions that matches the uptake pattern at bone scanning in *A*. *dWBS* = diagnostic WBS.

proven effect on survival in prostate cancer and lower hematologic toxicity (13).

### From Classic to Modern Theranostic Agents

More recently introduced theranostic agents include pharmaceuticals that target metastatic bone lesions, prostate cancer, and neuroendocrine tumors. These agents leverage advanced imaging technologies (SPECT/CT, PET/CT, PET/MRI) and are highly influenced by molecular biologic factors, extensively evidence based, and founded in a robust multidisciplinary approach to health care.

### Somatostatin Analog Radioligands

In previous years, options for the diagnosis and treatment of neuroendocrine tumors were scarce. This scarcity was due in part to the relative rarity of these neoplasms and consequently the lack of a market large enough to attract significant resources to identify specific treatments and diagnostic tools. This scenario changed at the end of the 20th century when clinicians gained understanding of the biologic behavior and functional and molecular characteristics of somatostatins. During the past decades, there has been a simultaneous unexplained rising incidence of neuroendocrine tumors, especially gastroenteropancreatic neuroendocrine neoplasms, which have increased from 10.9 to 52.4 cases per million tumors in the United States (23).

Somatostatin is an oligopeptide hormone normally encountered in the hypothalamus, nervous system, pancreas, and gastrointestinal tract (24). SSTRs have been found on various cells of neuroendocrine origin, including tumors, and somatostatin inhibits tumor cell growth. The understanding that certain types of neoplasms may overexpress SSTR dates back to the 1980s (25), and this insight later offered the opportunity to use radiolabeled somatostatin analog radioligands for theranostics.

The evolution toward a theranostic approach to diagnose and treat neuroendocrine tumors took a step forward in 1993, when the Rotterdam experience was published (24), with more than 1000 patients imaged with  $^{111}\text{In}$ -diethylenetriamine-pentaacetic acid octreotide ( $^{111}\text{In}$ -pentetetreotide [OctreoScan, Curium; London, England, and Paris, France]), a radiolabeled peptide for neuroendocrine tumor evaluation, staging, and characterization with scintigraphy. Later, in 1994, the U.S. Food and Drug Administration approved the use of OctreoScan as an imaging radiopharmaceutical owing to its higher sensitivity and specificity for gastroenteropancreatic neuroendocrine tumor evaluation compared with the sensitivity and specificity of conventional imaging.

Following use of the radioiodine prototype for thyroid cancer, the first peptide receptor radionuclide therapy (PRRT) procedures emerged in 1992, with very high doses of  $^{111}\text{In}$ -pentetetreotide used to explore a particular type of radioactive

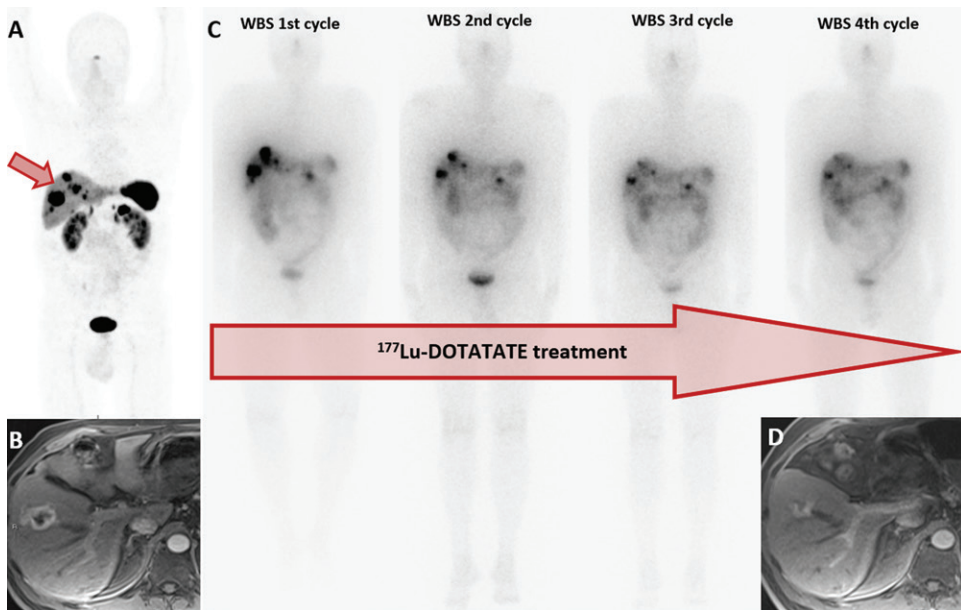


**Figure 9.** *A*, Coronal MIP  $^{68}\text{Ga}$ -DOTATATE PET/CT scan in a 56-year-old man with a known previous pancreatic neuroendocrine tumor and hepatic metastasis, obtained to assess disease status on the basis of SSTR expression, shows intense radiotracer uptake (arrow), such that the patient was allowed to receive  $^{177}\text{Lu}$ -DOTATATE therapy. *B–D*, The therapeutic effectiveness (partial response) can be observed on comparative axial MR images obtained before, *B*, and after, *D*, treatment and on anterior WBS scans, *C*, obtained immediately after each treatment cycle.

emission based on the Auger and conversion electrons of  $^{111}\text{In}$ . A few years later, DOTA–chelated peptides emerged, and in 1997, the first study of PRRT with  $^{90}\text{Y}$ -labeled DOTA—that is,  $^{90}\text{Y}$ -DOTATOC—was performed and showed the eradication of pancreatic neuroendocrine tumors in experimental rats (26).

Peptides are relatively simple, easily produced molecules that have fast clearance, rapid tissue penetration, and low antigenicity. With these advantages, the development of radiolabeled peptides for diagnostic and therapeutic applications in oncology, especially a variety of somatostatin analog ligands (27,28), thrived during the following decade, enabling the development of imaging radiotracers and targeted PRRT.

The emergence of  $^{68}\text{Ga}$ -labeled SSTR analogs ( $^{68}\text{Ga}$ -DOTATOC,  $^{68}\text{Ga}$ -DOTATATE, and  $^{68}\text{Ga}$ -DOTANOC) for PET, beginning in year 2000 (29), was a game changer for the imaging-based diagnosis, staging, and follow-up of neuroendocrine tumors.  $^{68}\text{Ga}$ -labeled SSTR analogs have several advantages, including improved image resolution and higher sensitivity and specificity, compared with scintigraphy and conventional imaging. These features have had a more significant effect on health care, improving clinician confidence and leading to lower costs, decreased imaging time, more rapid examination results, and lower radiation doses to patients. The body of evidence supporting the superiority of SSTR analog imaging has correspondingly grown expo-

nentially (30) and hence caused SSTR PET to rapidly gain in value, with a substantial increase in physician requests for and growing patient interest in this imaging modality (31).

Currently, SSTR PET is recommended in many guidelines and appropriate use criteria determined by multidisciplinary panels (32–34). Clinical scenarios considered appropriate for SSTR PET include initial disease staging; investigation of unknown primary tumors; and evaluation of lesions that are suggestive of neuroendocrine tumors but not suitable to biopsy, evaluation of patients with biochemical evidence and symptoms of neuroendocrine tumor, and evaluation of patients with biochemical evidence but no conventional imaging evidence of neuroendocrine tumor and no prior histologic diagnosis. Other applications include restaging of clinical or laboratory progression of disease without progression seen at conventional imaging, and evaluation of a newly discovered indeterminate lesion with unclear progression seen at conventional imaging (34).

**Rationale and Clinical Aspects.**—The theranostics approach for neuroendocrine tumors requires the integration of diagnostics and therapeutics by means of specific SSTR targeting with radiopharmaceuticals suitable for imaging or therapy. Molecular imaging for diagnosing and determining the extent of disease can enable effective planning and design of a treatment with use of the same or a similar targeting molecule (Figs 9, 10). This

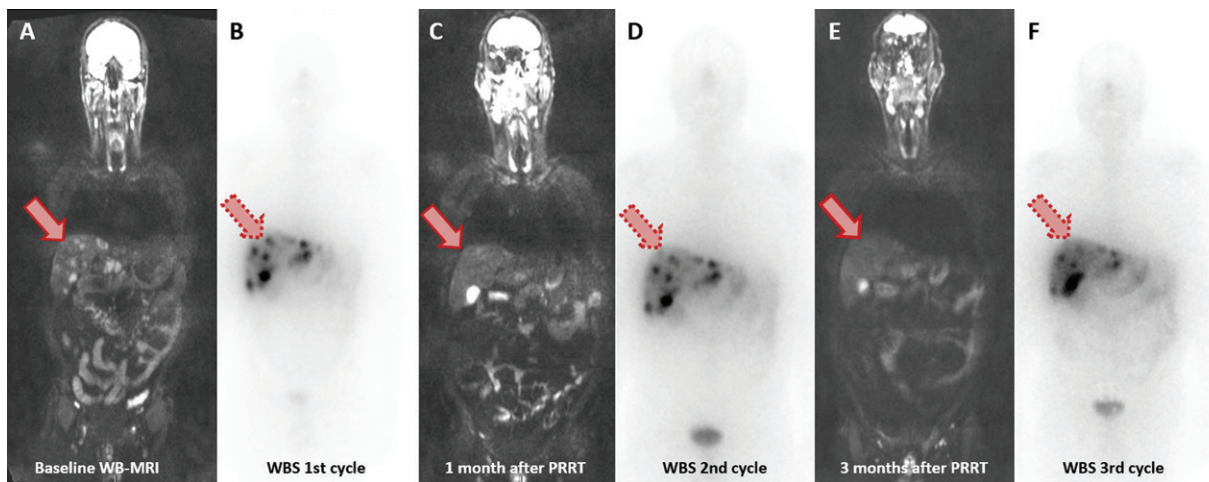


**Figure 10.** Glucagon- and gastrin-secreting neuroendocrine carcinoma of the pancreatic tail (Ki-67 index, 5%) and hepatic metastases (Ki-67 index, 1%) in a 49-year-old man. Follow-up  $^{177}\text{Lu}$ -DOTATATE images demonstrate the lesions' progressive response to the theranostic treatment. *A, C, E*, Coronal whole-body diffusion-weighted MR images, and *B, D, F*, anterior posttherapy  $^{177}\text{Lu}$ -DOTATATE WBS scans demonstrate the same treatment response pattern (arrow). This case exemplifies the treatment applications that are possible when other imaging modalities are integrated into the theranostic workup.

observation supports targeted radionuclide therapy with use of radiolabeled SSTR ligands, because no effective general antitumor treatment is available for metastasized neuroendocrine tumors, and only symptomatic relief can be achieved by using somatostatin analogs and interferon.

The design, choice, and implementation of PRRT should follow a joint clinical decision made by a multidisciplinary team. Patients suitable for the SSTR theranostics approach (35) have SSTR-positive well-differentiated or moderately differentiated neuroendocrine tumors, regarded as World Health Organization grade 1 or 2 neoplasms (36). Some authors (37,38) have suggested that patients who have grade 3 tumors but a Ki-67 index ranging from 20% to 50% may have SSTR expression high enough to warrant PRRT, but more research needs to be performed to confirm this. PRRT is currently indicated for patients with metastatic or inoperable neuroendocrine tumors, especially those who experience disease progression under SSTR agonists such as lanreotide.

Furthermore, PRRT is associated with improved clinical symptoms and disease control in patients with pheochromocytomas (39) and paragangliomas (40)—notably head and neck paragangliomas—and in individuals with tumors related to succinate dehydrogenase mitochondrial enzyme gene (*SDHx*) mutations (*SDHx*-related pheochromocytomas and paragangliomas). These improvements may also be seen in patients with sporadic hormone-secreting pheochromocytoma (39,41). Patients with metastatic neuroblastomas (42), medullary thyroid carcinomas (43), and even recurrent meningiomas (44) also may benefit from PRRT, provided

they meet the key criterion for theranostics: imaging demonstration of radiotracer uptake by the neoplastic lesions.

More than just an elegantly designed, tailor-made molecular approach, SSTR agonist PRRT has provided new hope for patients with metastatic neuroendocrine tumors. The excellent outcomes obtained with PRRT over the years have resulted in the rapid spread of this therapy throughout the world, with thousands of patients treated and increasing numbers of studies published, even before regulatory authorities approved the use of PRRT.

A part of the unparalleled developments in nuclear medicine theranostics during the past decade are due to the enormous response to the NETTER-1 study (45), a phase 3 randomized controlled trial encompassing 41 global sites. That study involved patients who had progressive well-differentiated metastatic midgut neuroendocrine tumors, with SSTRs present in all target lesions. Individuals were randomly assigned to undergo treatment with  $^{177}\text{Lu}$ -DOTATATE in addition to best supportive care (30 mg of long-acting repeatable [LAR] octreotide therapy), or a double dose (60 mg) of LAR octreotide only. PRRT with  $^{177}\text{Lu}$ -DOTATATE, as compared with treatment with a double dose of LAR octreotide, was associated with a statistically significant and clinically meaningful reduction (79%) in the risk of disease progression or death (45).

Moreover, patients in the  $^{177}\text{Lu}$ -DOTATATE arm reported prolonged maintenance of global health status, a longer time to deterioration across multiple clinically relevant symptom categories, and a longer period of sustained functional health-related quality of life (46).

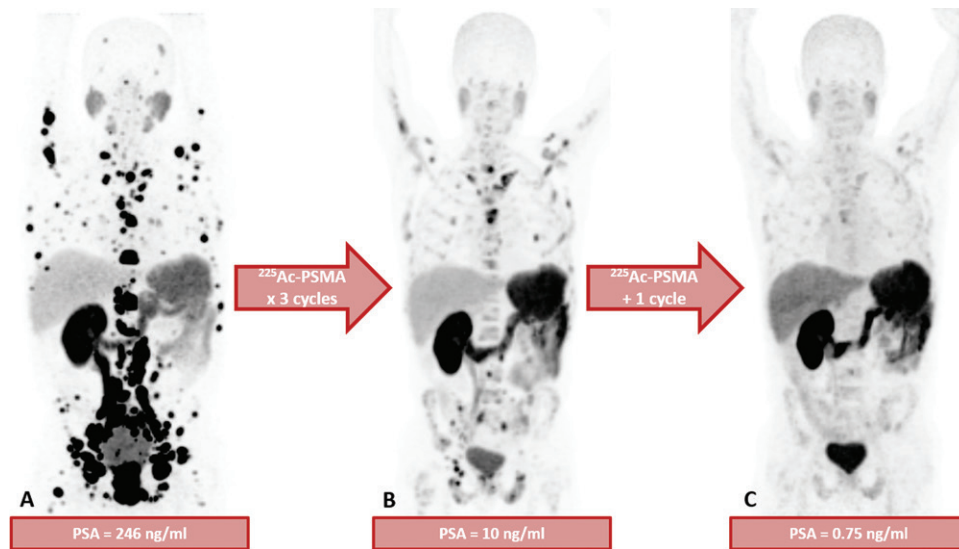


**Figure 11.** Theranostic approach in a patient with mCRPC who was treated with several cycles of  $\alpha$ -particle-emitter <sup>225</sup>Ac-PSMA therapy. *A*, Coronal MIP <sup>68</sup>Ga-PSMA PET/CT scan shows high PSMA expression in many metastatic lesions, making them a reachable target. *B*, *C*, Coronal follow-up MIP <sup>68</sup>Ga-PSMA PET/CT scans after three therapy cycles, *B*, and then after one additional cycle, *C*, show a partial response and the effectiveness of therapy.

Therefore, the NETTER-1 trial results provided indisputable proof of the positive effects of PRRT in the treatment of neuroendocrine tumors and led to this treatment being approved by the U.S. Food and Drug Administration.

There is debate regarding the use of <sup>90</sup>Y and/or <sup>177</sup>Lu for PRRT used as single agents or in combination, because preliminary studies have indicated that larger tumors respond better to <sup>90</sup>Y, whereas smaller ones respond better to <sup>177</sup>Lu PRRT. Nonetheless, the actual benefit of using a combined variant of PRRT in humans with gastroenteropancreatic neuroendocrine tumors remains unknown, although the potential efficacy has been reported (47–49).

### PSMA Radioligands for Prostate Cancer

Prostate cancer is the most common noncutaneous cancer in males. It is the third leading cause of cancer deaths among men in the western hemisphere. Despite the good prognosis for individuals with disease in its early stages, the prognosis is poor for those with metastatic disease, for whom the 5-year survival rate is approximately 29% (50). Depending on the clinical stage of their cancer, up to 65% of patients may experience recurrence marked by biochemical failure, with a subsequent higher risk for progression to castration-resistant metastatic prostate cancer (mCRPC).

The introduction of PSMA PET has revolutionized the evaluation of prostate cancer. The high expression of PSMA, a glycoprotein, in prostate cancer cells makes it an optimal imaging target. The high capability of PSMA PET for depicting diminutive, previously undetected lesions has been widely demonstrated in the literature and has led to a rethinking regarding patient management among oncologists, urologists, and radiation oncologists (51).

mCRPC refers to the distant spread of prostate cancer, even in patients who are being treated with androgen deprivation therapy and/or surgical castration. It may affect up to 20% of patients with prostate cancer and portends a poor prognosis, with affected patients having an average survival of 19 months (52). This scenario has prompted the development of theranostic agents with molecules binding to PSMA (53), the aim being to obtain results similar to those obtained for neuroendocrine neoplasms.

**Rationale and Clinical Aspects.**—The unique features of PSMA radiotracers for assessing key molecular phenotypes with higher sensitivity, specificity, and target-to-background ratio facilitate better diagnostic accuracy compared with that achieved with the modalities previously used to address prostate cancer recurrence (54–56). These features offer new possibilities for reducing the critical gap between recurrences that are detectable with prostate-specific antigen only and imaging-detectable recurrences, as well as a new way of looking at disease spread.

The diagnosis of metastatic disease with use of PSMA PET enables detection of tumor burden and establishes a baseline for future response assessment. Moreover, it serves as a theranostic selector for radionuclide PSMA-based therapy (Fig 11) (57,58). Owing to these attributes, the potential of PSMA binders as imaging and therapeutic agents has been extensively investigated in several centers around the world, with thousands of treatment cycles having been administered and yielding promising dosimetric, safety, and efficacy data (59).

Various molecules that are capable of binding to PSMA can be used for PSMA-targeted radioligand therapy (PRLT) in patients with mCRPC

(60). These molecules have two main components. The first component is a small peptide belonging to the class of glutamine-urea-lysine analogs, which are molecules capable of connecting to the extracellular domain of the PSMA transmembrane protein and then undergoing internalization into the intracellular environment (60). The second component is an emitter (most frequently  $^{177}\text{Lu}$  and  $^{225}\text{Ac}$ ), which, after cell internalization, delivers radiation to the nucleus of tumor cells, promoting DNA damage (61).

The effectiveness of PRLT with  $^{177}\text{Lu}$ -PSMA has been investigated in several studies (62–64), with high response rates and a low toxicity profile demonstrated. PRLT promotes the reduction of prostate-specific antigen levels in most patients and has a significant effect on the quality of life of men who have mCRPC that has progressed after conventional treatment. These men have had considerable reductions in pain and improved performance status parameters. Overall survival is significantly higher in patients who respond to the first cycle of PRLT (68 weeks) than in nonresponders (33 weeks), regardless of the magnitude of the response (65). Also, in terms of imaging-depicted response to PRLT, according to the Response Evaluation Criteria in Solid Tumors (RECIST) version 1.1 data, this therapy is associated with notable rates of partial response and stable disease (66). Finally, there is also evidence of increased survival (29.4 weeks) among patients who receive PRLT as compared with the survival from historic retrospective data (19.7 weeks) on patients who received the best therapeutic support care (67). Therefore, prospective studies involving larger populations are necessary to confirm the usefulness of PRLT reported in earlier scenarios, especially considering the scarcity of effective therapeutic modalities and the poor prognosis for patients with mCRPC.

### Bone-seeking Agents Revisited

A revival of the use of radioisotopes to treat bone metastasis occurred after the establishment of  $^{223}\text{Ra}$ -dichloride (or simply  $^{223}\text{Ra}$ ) as a treatment that has a positive effect on both symptoms and survival. An  $\alpha$ -particle emitter,  $^{223}\text{Ra}$  has been systematically used for treatment of bone metastases derived from prostate cancer. It is a calcium analog with a half-life of 11.4 days, which is ideal for radioisotopic therapy (13,68,69).

The mechanism of  $^{223}\text{Ra}$  uptake is similar to that described for  $^{186}\text{Re}$ -HEDP,  $^{188}\text{Re}$ -HEDP, and  $^{153}\text{Sm}$ -EDTMP uptake and essentially the same as that of strontium 89 ( $^{89}\text{Sr}$ ) (ie, strontium chloride) uptake.  $^{223}\text{Ra}$  and  $^{89}\text{Sr}$  are calcium analogs that are deposited in areas of intense bone matrix formation, as is the case with osteoblastic lesions.

However, the shorter range and much higher energy (and thus higher radiation dose delivered) of the  $\alpha$ -particle emission favor the effectiveness of treatment with  $^{223}\text{Ra}$ . The result is better outcomes such as less bone marrow toxicity and increased survival in patients with mCRPC; thus, two marked limitations of  $^{186}\text{Re}$ -HEDP-,  $^{188}\text{Re}$ -HEDP-,  $^{89}\text{Sr}$ -, and  $^{153}\text{Sm}$ -based treatments are overcome (13,68).

Because treatment with  $^{223}\text{Ra}$  began during the era of evidence-based medicine, there is significant prospective data to support its use. The results of a randomized phase 3 trial involving 921 patients confirmed that treatment with  $^{223}\text{Ra}$  for mCRPC resulted in higher overall survival rates (gain of 3.6 months of median overall survival) in patients without visceral metastasis. Also, a reduction in adverse events, including less necessity for analgesic localized radiation therapy, fewer pathologic fractures, and fewer orthopedic interventions overall, compared with adverse events in the placebo group, was seen. Almost all outcomes of the trial were favorable, and follow-up studies confirmed the results (70).

Nevertheless,  $^{223}\text{Ra}$  does not provide enough fractional  $\gamma$ -ray emissions and is therefore not favorable for routine posttherapy imaging. In this sense, bone scintigraphy (regular bone scintigraphy with  $^{99m}\text{Tc}$ -marked bisphosphonates or  $^{18}\text{F}$ -sodium fluoride PET/CT) remains necessary to predict uptake of the isotope by metastatic lesions.

In terms of the future, there are still uncertainties regarding the ideal time during the course of the disease to start using  $^{223}\text{Ra}$  (71). In addition, it is unclear whether a combination of  $^{223}\text{Ra}$  treatment with other modalities, such as new-generation hormone therapies (eg, enzalutamide), chemotherapy, and immunotherapy, results in better or worse outcomes (71,72). Finally, if and when  $^{223}\text{Ra}$  therapy should be combined with other radioisotopic therapies such as PSMA-based treatments that are yet to be tested, and the use of  $^{223}\text{Ra}$  in tumors other than prostate cancers, are still under investigation (13).

### Hepatic Radioembolization

Hepatic radioembolization for primary or metastatic liver lesions is a multistep multidisciplinary theranostic procedure involving planar scintigraphy, SPECT/CT, CT, MRI, PET/CT/MRI, arteriography, and judicious clinical evaluation.

The rationale for radioembolization is the delivery of therapeutic radioisotopes (in the form of microspheres) to tumors by accessing their neoplastic microarterial vasculature. Since an arterial neovasculature preferably supplies most hepatic tumors rather than the healthy parenchyma, which is predominantly supplied

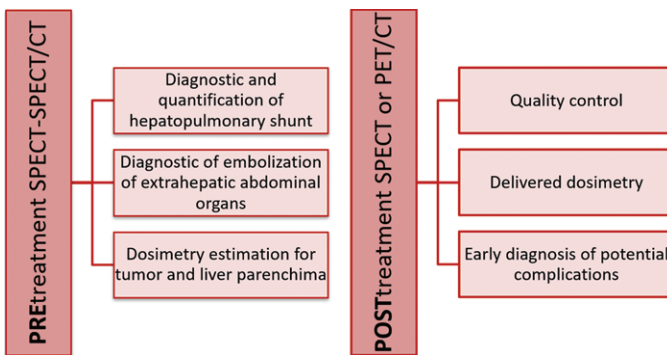


**Figure 12.** Diagram illustrates the indications and advantages of pretreatment SPECT combined with fused SPECT/CT, and posttreatment SPECT or fused PET/CT for theranostic hepatic radioembolization.

by the portal vein, the hepatic arterial route is a reasonable target by which to reach these lesions selectively. Most of the radioactive microspheres currently available are made of glass or resin and based on  $^{90}\text{Y}$ , a high-energy  $\beta$ - and  $\gamma$ -particle-emitting radioisotope with high tissue-damaging potential. Thus, placing microspheres exactly in the tumor region is critical, as it allows delivery of high radiation doses to the tumor and a lower radiation dose to the healthy parenchyma, and it helps avoid embolization and/or irradiation of nontarget abdominal structures. Even more important, accurate microsphere placement helps prevent leakage of radioactive microspheres into the systemic venous circulation, culminating in lung microvascular embolization.

Because the target pathway in radioembolization is not a specific molecular but rather a mechanical pathway, an imaging component that simulates the microsphere distribution after arterial injection is mandatory.  $^{99\text{m}}\text{Tc-MAA}$  scintigraphy fulfills this role since MAA particles have physical characteristics similar to those of microspheres (especially size, on the order of micrometers). Processes such as pulmonary embolization resulting from intrahepatic arteriovenous shunt placement and embolization of abdominal extrahepatic structures due to anatomic variations in arterial supply, as well as the relationship between tumoral and healthy parenchyma arterial perfusion, can be predicted by using scintigraphic planar and hybrid (SPECT/CT) techniques, enhancing the safety of the procedure (73). In addition,  $^{99\text{m}}\text{Tc-MAA}$  scintigraphy can provide tumor absorbed dose estimations, enabling optimal activity of the administered radiopharmaceutical in each patient (Fig 12).

However, planning scintigraphy cannot be performed alone, without planning arteriography, which is an essential step not only for  $^{99\text{m}}\text{Tc-MAA}$  injection but also for initial assessment of the vascular anatomy and the associated implications in the procedure. Moreover,  $^{90}\text{Y}$   $\gamma$ -ray and positron emissions can yield an immediate image (SPECT or PET) of injected microspheres, al-

lowing quality control of the procedure in terms of the placement of microspheres in the liver, early diagnosis of extrahepatic foci of radiopharmaceutical accumulation, and calculation of the effective radiation dose delivered to the tumor(s) (Fig 13). As with other modern theranostic procedures, there is a strong and growing body of evidence supporting the use of hepatic radioembolization for select indications—for example, to treat hepatocellular carcinoma, colorectal cancer, and neuroendocrine tumors (74).

### FDG: The Antitheranostic Agent?

$^{18}\text{F}$ -fluorodeoxyglucose (FDG) PET and PET/CT have revolutionized the diagnosis and management of various types of cancer, inflammatory and infectious conditions, and neurologic diseases (75–78). FDG PET/CT has helped to more closely integrate molecular imaging into medical practice, especially oncology, since FDG PET/CT can provide *in vivo* and whole-body imaging of a molecular feature that is common for most cancer types: the glycolytic pathway. Glycolysis has a central role in carcinogenesis, cancer cell survival, and proliferation of most cancer types, being recognized as a cancer hallmark and potential target for antitumoral therapy (79). Changes in cellular machinery to transform normal glucose metabolism (oxidative phosphorylation) into aerobic glycolysis represent a well-described phenomenon that occurs in neoplastic cells known as the Warburg effect (80). FDG PET has capability to depict and quantify the *in vivo* glucose uptake by neoplastic cells, generating diagnostic, prognostic, and follow-up parameters that are highly correlated with tumoral activity; this process has been extensively studied. Higher FDG uptake rates are associated with more aggressive and undifferentiated tumor phenotypes and a poorer prognosis for many cancers (81).

On the other hand, most of the theranostic procedures discussed earlier in this article are directed against specific cell phenotypes that generally require a degree of differentiation sufficient

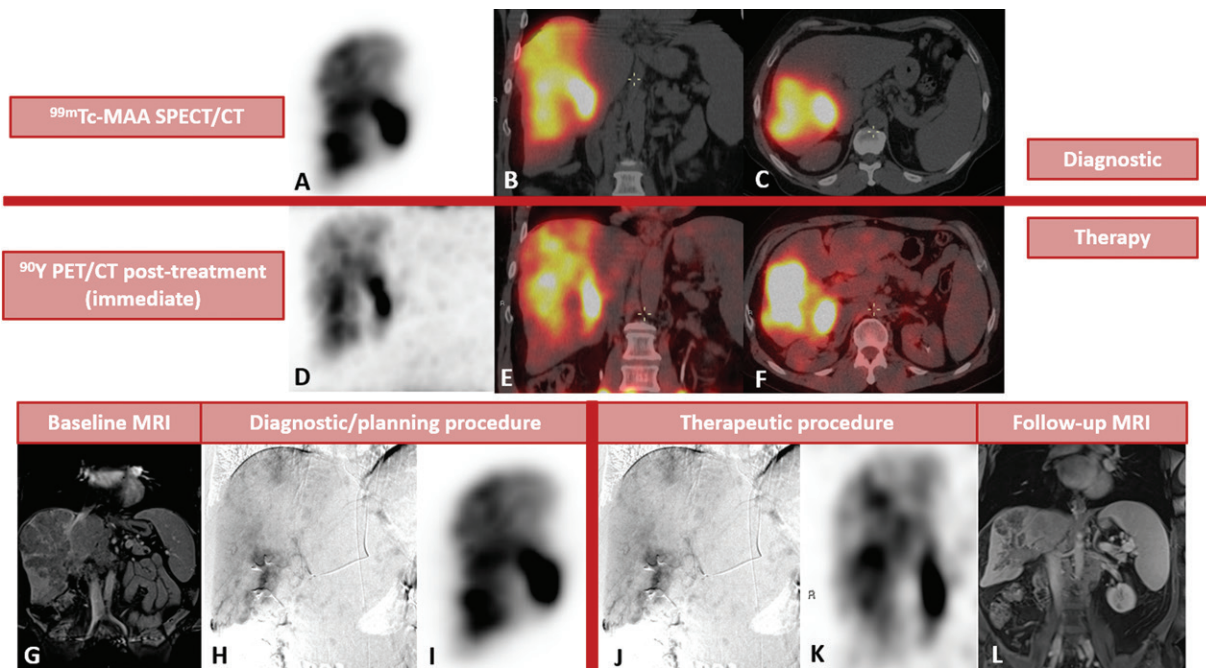


**Figure 13.** Importance of pretreatment imaging for hepatic radioembolization with  $^{90}\text{Y}$  microspheres. A–C, I, Anterior coronal  $^{99}\text{mTc}$ -MAA scintigrams, A, I, and coronal, B, and axial, C, fused  $^{99}\text{mTc}$ -MAA SPECT/CT scans, with  $^{99}\text{mTc}$ -MAA injected intra-arterially, can be used to predict the behavior of injected  $^{90}\text{Y}$  microspheres. D–F, Subsequent anterior coronal posttreatment  $^{90}\text{Y}$  PET image, D, and coronal, E, and axial, F, PET/CT images reveal a matching pattern, confirming the accuracy of pretreatment imaging analysis of the distribution, extrahepatic accumulation (source of potential toxicity), and estimation of absorbed doses (prediction of response) to the tumor. G, Coronal T1-weighted contrast-enhanced abdominal MR image depicts extensive hepatic involvement by tumor lesions. H, Anterior hepatic arteriogram for treatment planning reveals the rich blood supply to the lesions. During arteriography,  $^{99}\text{mTc}$ -MAA was injected through an arterial catheter, allowing an anterior coronal  $^{99}\text{mTc}$ -MAA scintigram, I, to be obtained. With these image features, hepatic radioembolization with  $^{90}\text{Y}$  microspheres was planned and performed a week later. J, Another anterior hepatic arteriogram was obtained, allowing the intra-arterial injection of  $^{90}\text{Y}$  microspheres. K, Axial posttreatment  $^{90}\text{Y}$  PET image shows radioembolization of the lesions. L, Coronal follow-up contrast-enhanced T1-weighted abdominal MR image shows radiation-induced tumor shrinkage.

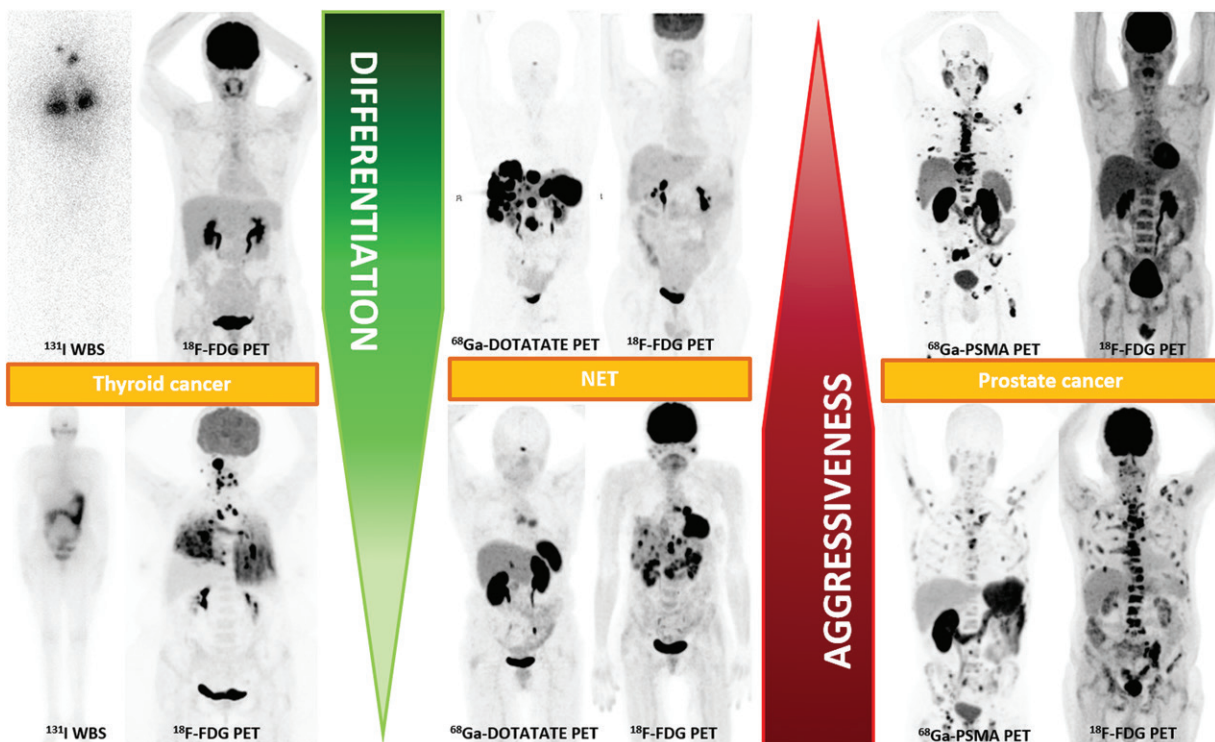


**Figure 14.** Role of FDG as an antitherapeutic agent in thyroid, prostate, and neuroendocrine (NET) tumors depicted on anterior  $^{131}\text{I}$  WBS and anterior MIP PET scans. Note the inverse relationship between tumor differentiation (green) and aggressiveness (red) and the relationship of these features to FDG uptake: The greater the FDG uptake, the less differentiated and more aggressive the tumor tends to be.

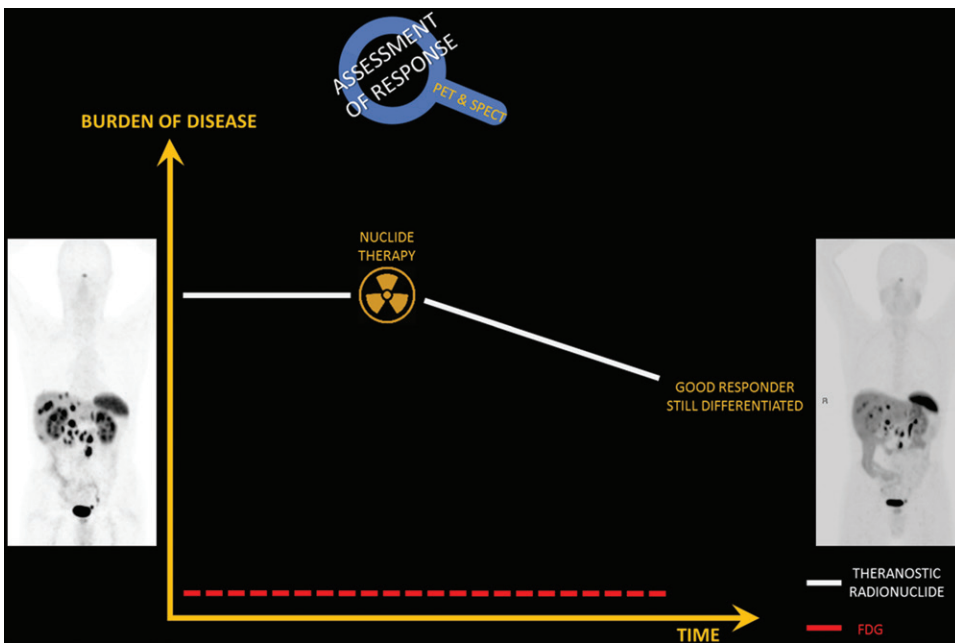


**Figure 15.** Diagram illustrates burden of disease over time, assessed at PET with use of the theranostic radionuclide and FDG. In this example, a patient with a well-differentiated metastatic neuroendocrine tumor had a good response to radionuclide therapy, depicted on coronal MIP  $^{68}\text{Ga}$ -DOTATATE PET scans. FDG PET was not performed, as it was not considered with relevant burden of undifferentiated tumor phenotypes.

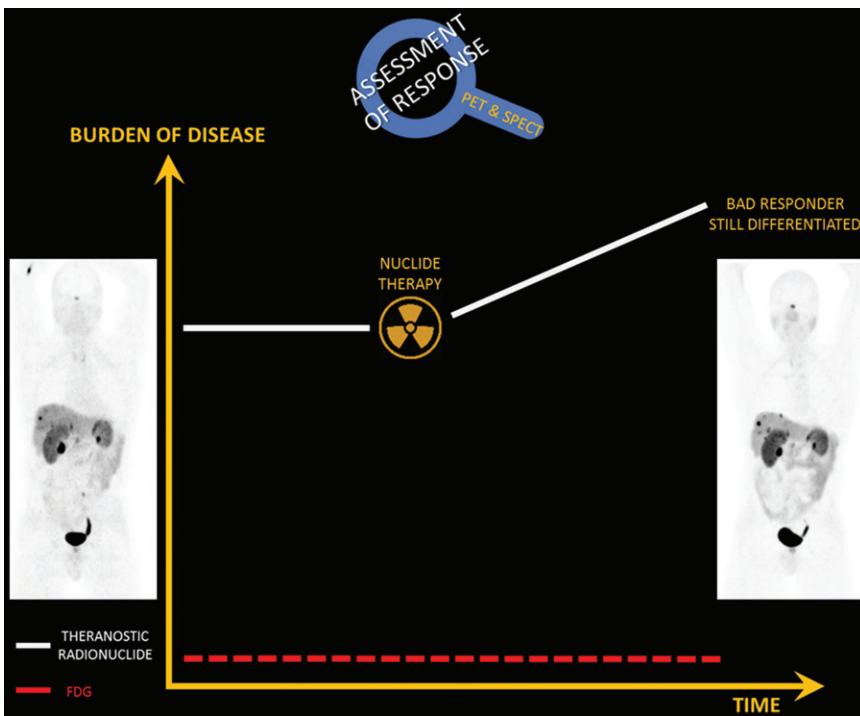


**Figure 16.** Diagram illustrates burden of disease over time, assessed at PET with use of the theranostic radionuclide and FDG. This example illustrates a case of poor treatment response. The patient has a metastatic neuroendocrine tumor, as depicted on coronal MIP  $^{68}\text{Ga}$ -DOTATATE PET scans before (left) and after (right) radionuclide therapy. Scans reveal increasing burden of still-differentiated disease, even after radionuclide therapy. FDG PET was not performed, as it was not considered with relevant burden of undifferentiated tumor phenotypes.

to be satisfactorily expressed and consequently targeted (Fig 14). Thus, tumor differentiation and aggressiveness are important parameters that influence theranostic efficacy at the beginning or during the middle of treatment owing to the specific tumor clonal predominance (Figs 15–18). In this context, FDG PET has a pivotal role in the theranostic approach, enabling better patient

selection through characterization of more undifferentiated and/or aggressive phenotypes, and avoiding ineffective, potentially toxic, and costly treatments. There is evidence supporting the incorporation of FDG PET into some theranostic algorithms to detect clonal selection and/or undifferentiation or to characterize unfavorable theranostic indications (Table 3) (82).

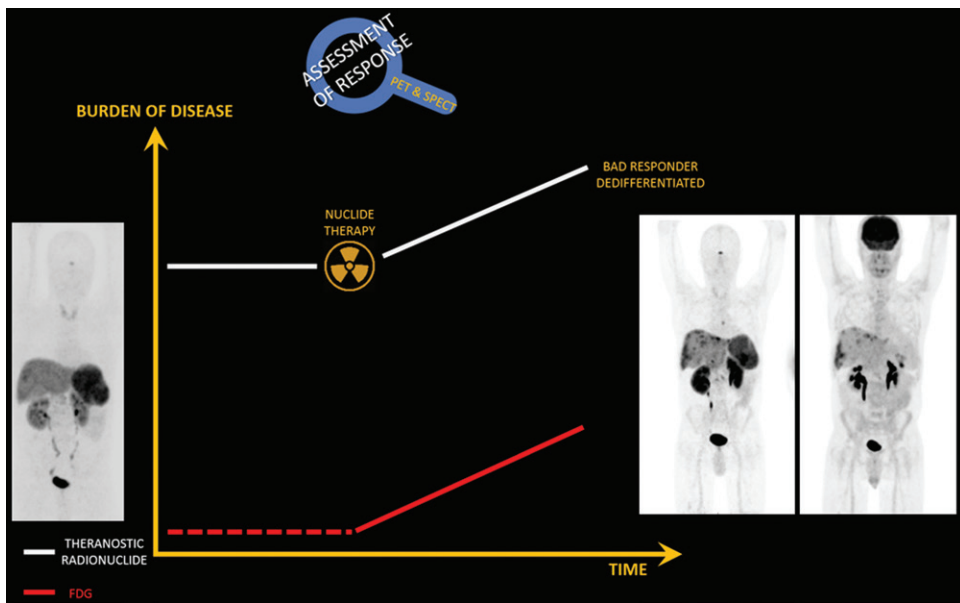


**Figure 17.** Diagram illustrates burden of disease over time, assessed at PET with use of the theranostic radionuclide and FDG. In this example of poor treatment response, baseline coronal MIP  $^{68}\text{Ga}$ -DOTATATE PET scan (far left) shows hepatic lesions from a metastatic neuroendocrine tumor. After radionuclide therapy, coronal MIP  $^{68}\text{Ga}$ -DOTATATE PET scan (left image in right set) shows new lesions and increases in the intensity and extension of tracer uptake by previous lesions. Coronal MIP FDG PET image (far right image) shows increasing burden of dedifferentiated disease (high FDG uptake) after radionuclide therapy.

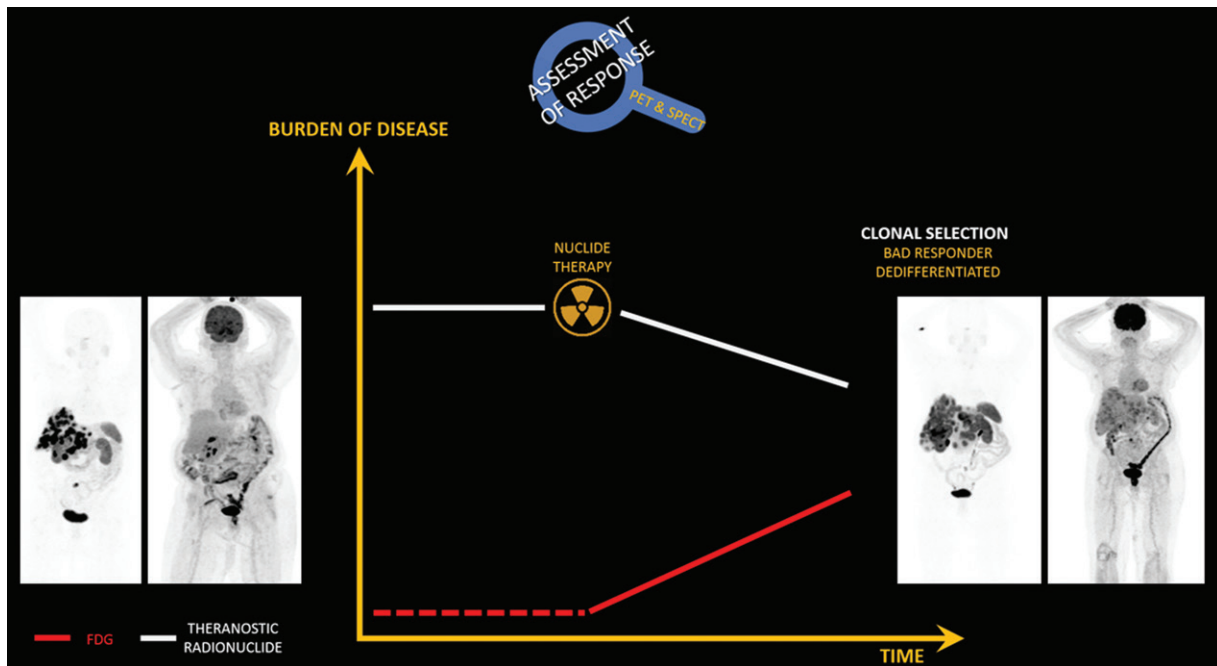


**Figure 18.** Diagram illustrates burden of disease over time, assessed at PET with use of  $^{68}\text{Ga}$ -DOTATATE (left image in both sets) and FDG (right image in both sets). In this case, the patient had poor treatment response with clonal selection. Compared with the pretreatment coronal PET scans (images at left), coronal MIP interval PET scans (images at right) show the well-differentiated metastatic neuroendocrine tumor with decreased burden of disease, manifesting as lower uptake at  $^{68}\text{Ga}$ -DOTATATE PET after treatment (left) and increased burden of dedifferentiated disease with high uptake at FDG PET after radionuclide therapy (right).

However, clinical practice has demonstrated that for most of the diseases suitable for theranostic applications in nuclear medicine, only a

part of the cases involve “pure” differentiated or undifferentiated phenotypes, perhaps representing the extremes of the complex spectrum of

**Table 3: Roles of FDG in Different Clinical Settings**

Neoplasm	Theranostic Approach or Agent Pairing	Clinical Setting	FDG Indication (with Reference Numbers)
Differentiated thyroid cancer	$^{123}\text{I}$ WBS, $^{131}\text{I}$ radioiodine treatment	Undifferentiated or non-iodine-avid disease, prognostication	Rising thyroglobulin level ( $>10 \text{ ng/mL}$ ) $^{123}\text{I}$ WBS negative (14)
Neuroendocrine tumors	$^{68}\text{Ga}$ -DOTATATE, $^{177}\text{Lu}$ -DOTATATE	Disease heterogeneity or undifferentiation, prognostication	Ki-67 index, $>10\%$ Grade 3 neuroendocrine carcinoma Selection for PRRT (82)
Prostate cancer	$^{68}\text{Ga}$ -PSMA, $^{177}\text{Lu}$ -PSMA	Disease heterogeneity or undifferentiation, suspected neuroendocrine transformation	Selection for PRLT Rapid progressive disease

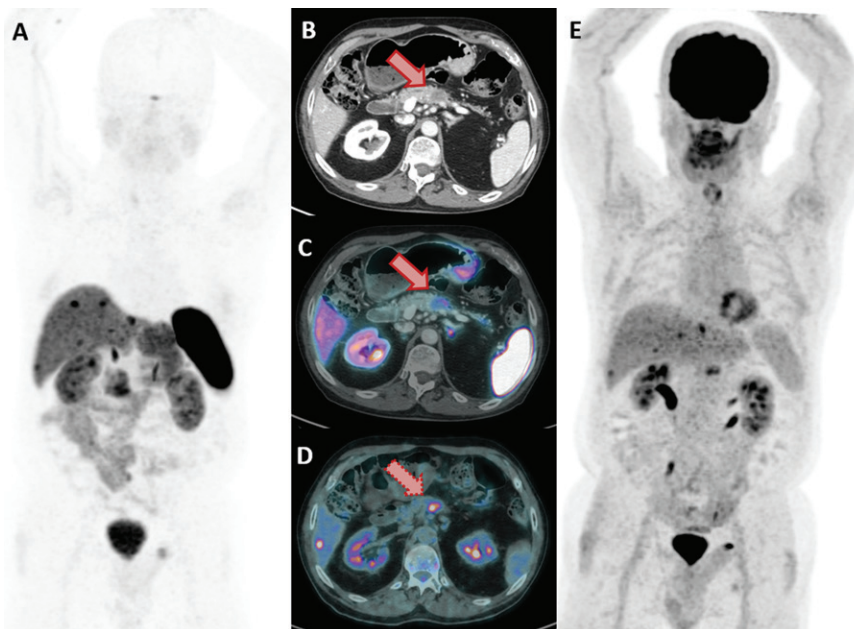


**Figure 19.** Tumor heterogeneity in an 81-year-old patient with metastatic pancreatic neuroendocrine cancer (Ki-67 index, 29%). *A–C*, Coronal MIP, *A*, axial contrast material-enhanced CT, *B*, and fused  $^{68}\text{Ga}$ -DOTATATE PET/CT, *C*, images show a hypovascular primary lesion (arrow in *B* and *C*) with low somatostatin expression. *D*, *E*, Axial fused, *D*, and coronal MIP, *E*, FDG PET/CT scans show hypermetabolism (arrow in *D*) that matches that of the predominant high-grade primary lesion. The molecular phenotype of a more aggressive lesion (higher uptake at FDG PET/CT than at  $^{68}\text{Ga}$ -DOTATATE PET) matches the morphologic aspect (hypovascular, with distal ductal dilatation and parenchymal atrophy) of the primary lesion.

tumoral differentiation. In this setting, an important concept emerges: tumoral heterogeneity. Tumoral heterogeneity is a broad and sometimes imprecise concept that can be related to differences in key phenotypes, genotypes, and cellular microenvironment interactions for a given type of tumor, ranging from intratumoral to interpatient (or even interpopulation) levels. Despite some vagueness in its definition, tumor heterogeneity for some features, such as differentiated (ie, theranostic targetable) and undifferentiated (ie, predominant glycolytic), has a potential effect on the behavior, diagnosis, therapeutic planning, response patterns, and outcomes of many

tumors. Again, FDG PET can provide valuable complementary information, revealing, for example, different grades of glycolytic metabolism and aggressiveness in the same patient (Fig 19). Clinical situations like this are sometimes challenging; however, they offer many possibilities for sequencing—and potentially combining—theranostic and conventional therapies (Fig 20).

Emerging data have confirmed the potential of FDG PET to improve theranostic selection by means of tumoral heterogeneity assessment. Interestingly, investigators in a recent study (83) proposed the use of a systematized grading score, derived by using a dual PET radiotracer (FDG

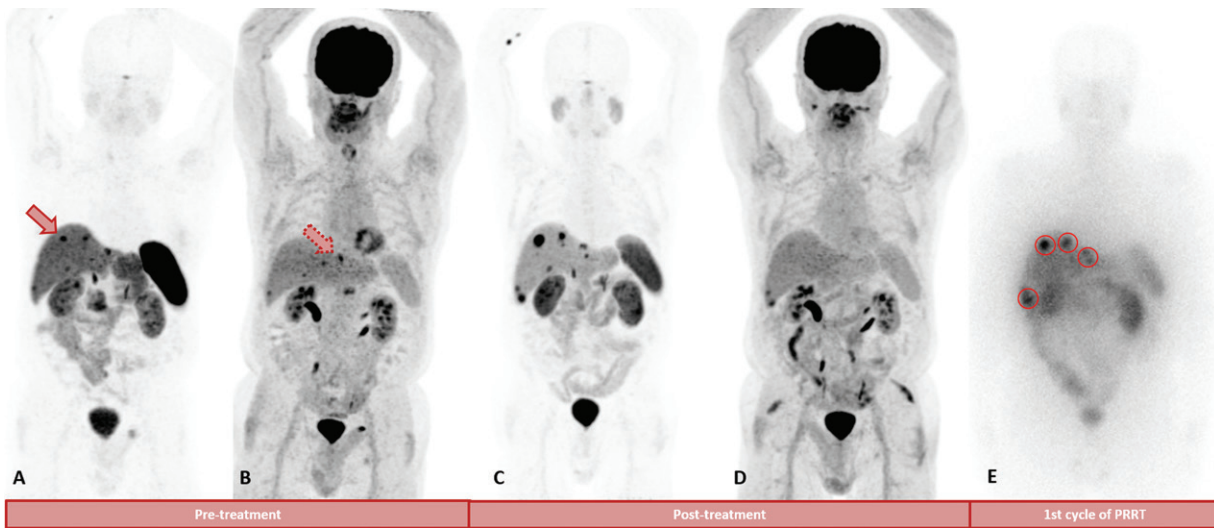


**Figure 20.** Selection of treatment, guided by molecular imaging, in an 81-year-old patient with metastatic pancreatic neuroendocrine cancer (Ki-67 index, 29%) (same patient as in Figure 19). *A, B*, Pretreatment coronal  $^{68}\text{Ga}$ -DOTATATE MIP, *A*, and FDG PET/CT, *B*, images show liver metastases (arrow) with different phenotypes. In the setting of FDG-avid lesions, a decision to add chemotherapy to the treatment plan was made. *C, D*, After 5 months of treatment, coronal  $^{68}\text{Ga}$ -DOTATATE MIP PET/CT scan, *C*, shows progression of the well-differentiated liver lesions, and coronal MIP FDG PET scan, *D*, shows partial response of the less-differentiated hepatic metastases. This response pattern led to the patient undergoing PRRT. *E*, Coronal posttherapeutic WBS scan shows effective delivery of the therapeutic radionuclide to the target lesions (red circles).

and  $^{68}\text{Ga}$ -DOTATATE), to stratify neuroendocrine tumors. Despite promising results with use of qualitative (uptake vs nonuptake) and simple semiquantitative ( $\text{SUV}_{\max}$ ) parameters, approaches such as whole-body and tumor burden quantification, radiomics, and other big data–based analyses are anxiously awaited. These methods may raise theranostics to the next level in terms of disease characterization and prognostication.

To summarize, FDG PET is not really an “antitheranostic” agent. Conversely, in a figurative way, this examination can act as a gatekeeper for radionuclide therapy. The antagonistic role of FDG PET in depicting undifferentiated and/or aggressive phenotypes is a valuable allying function. It may ultimately improve the performance of the theranostic approach, enabling better selection of patients and better understanding of the biologic behavior of the lesions.

## Advantages and Limitations of Theranostics

### Advantages

Better patient selection, capability for predicting response and toxicities (Fig 21), and prognostic power are obvious advantages of theranostic approaches. These features also represent new capabilities for imaging (especially hybrid imaging). They must be included in the roles of nuclear medicine physicians and nuclear radiologists, who should broaden their perspectives beyond diagnosis, altering their way of thinking in the current era of personalized medicine.

Clear advantages of theranostics in nuclear medicine include the possibility for whole-body imaging, ease of quantification, and combination of different radiotracers, enabling comprehensive assessment of biologic behavior and phenotypic tumoral heterogeneity. Moreover, these capabilities help to provide more powerful and precise tools for measuring the disease burden from each of the studied phenotypes. Sampling uncertainties, which are relatively common when considering tissue biopsy specimens, tend to decrease with whole-body molecular imaging. The ultimate benefits are a reduction in costs and the avoidance of potentially unnecessary treatments and interventions. As an example, studies of PET (84) show the potential advantage of anti-HER2 whole-body PET as compared with the current immunohistochemistry stain approach for breast cancer.

### Limitations

Theranostic pairs in nuclear medicine are not perfect magic bullets, and, thus, theranostic approaches have drawbacks. The sensitivity and specificity of the diagnostic tools (planar scintigraphy, SPECT, and PET) are limited, like those of all other diagnostic modalities, and thus have the potential to lead to erroneous selection of patients in some instances. This could result in the exclusion of patients who might respond to a specific treatment if imaging-based selection criteria were adopted. These limitations are based mainly on imaging system parameters such as spatial resolution and contrast resolution (Fig 22).

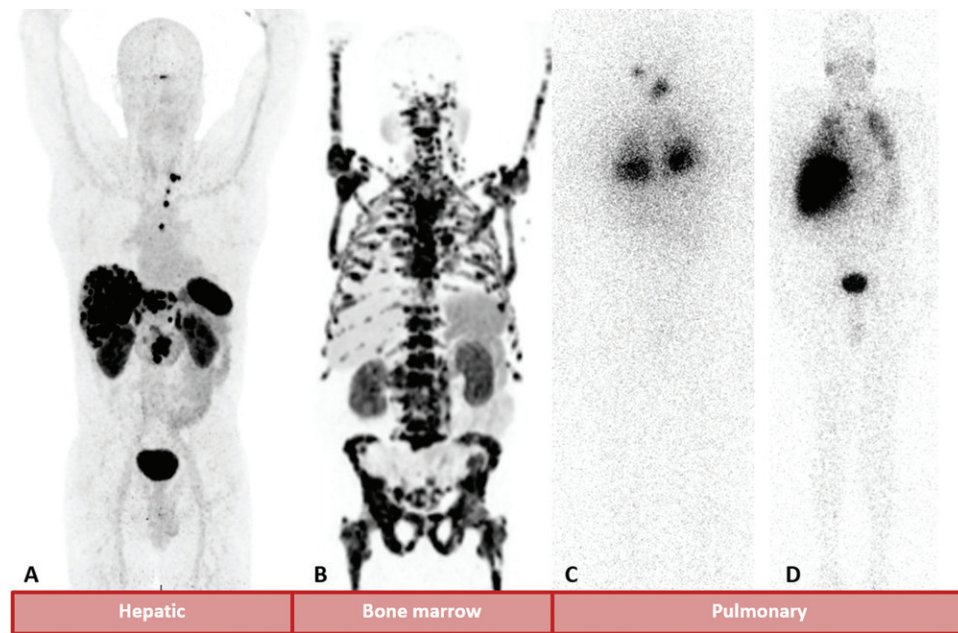


**Figure 21.** Prediction of toxicity based on the diagnostic component of theranostics. *A*, Coronal  $^{68}\text{Ga}$ -DOTATATE MIP/CT scan shows a high burden of hepatic disease. *B*, Coronal  $^{68}\text{Ga}$ -PSMA MIP scan shows diffuse infiltration of bone marrow. *C*, Anterior planar  $^{131}\text{I}$  WBS scan shows diffuse anomalous uptake in the lungs. *D*, Anterior planar WBS scan, with  $^{99\text{m}}\text{Tc}$ -MAA injected intra-arterially into the liver, shows a hepatopulmonary shunt with diffuse uptake in the lungs.

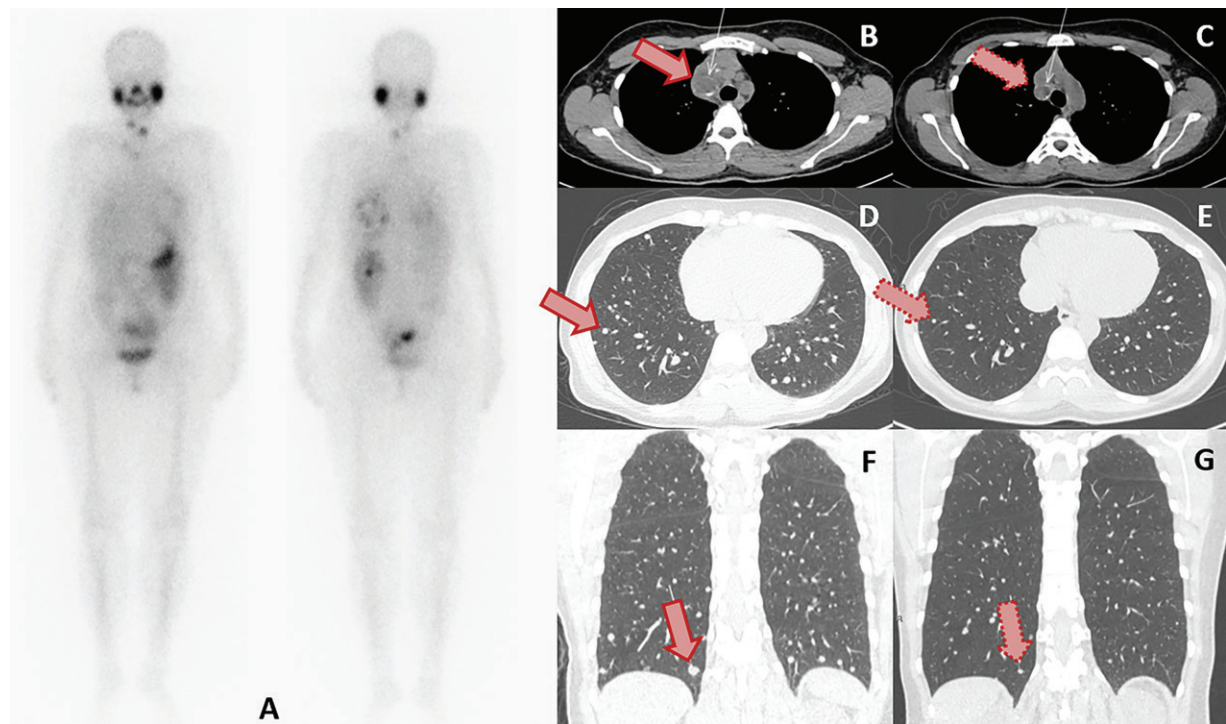


**Figure 22.** *A–C*, Dissociation between low  $^{131}\text{I}$  uptake on anterior (left) and posterior (right) WBS scans, *A*, and marked partial response on axial CT scans, *B*, *C*, of a mediastinal lymph node before (arrow in *B*) and after (arrow in *C*) radioiodine therapy. *D–G*, Axial, *D*, *E*, and coronal, *F*, *G*, CT scans show lung nodules before (arrow in *D* and *F*) and after (arrow in *E* and *G*) radioiodine therapy. This case illustrates a limitation of theranostics: exclusion of a patient who is a potential responder to therapy owing to low sensitivity of the diagnostic component.

On the other hand, the specificity of the therapeutic component of theranostic pairs is not perfect, as it is impossible to deliver radiation

to only the target lesions and avoid compromising adjacent nontarget tissues (Figs 23, 24). To reduce this shortcoming, it may be beneficial to

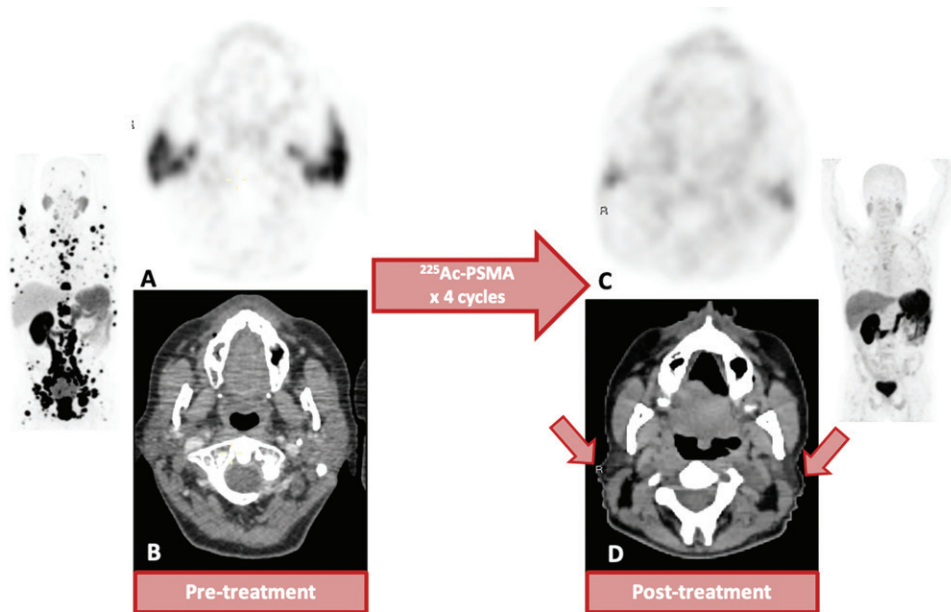


**Figure 23.** Salivary gland toxicity in a theranostic approach used in a patient who had metastatic prostate cancer and was treated with  $^{225}\text{Ac}$ -PSMA radioligand therapy. Axial pretreatment PET (top) and CT (bottom) images, A, B, and posttreatment PET (top) and CT (bottom) images, C, D, show reduced  $^{68}\text{Ga}$ -PSMA ligand uptake in the parotid glands and atrophy with fat deposition (arrows in D). Coronal MIP PSMA PET images demonstrate high tumor burden (far left PET scan) and substantial treatment response (far right PET scan).

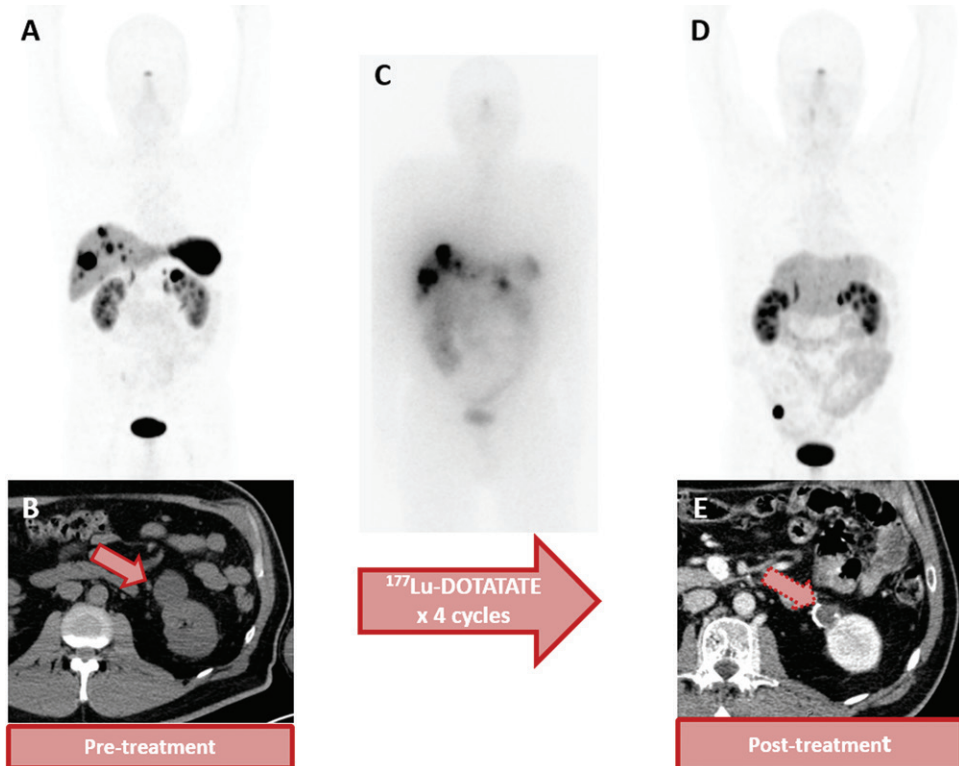


**Figure 24.** Radiation-induced atrophy in an exophytic cortical cyst (arrow in B and E) in the left kidney. This case illustrates how nontarget areas may be affected by radiation of neighboring structures. A, Coronal pretreatment MIP  $^{68}\text{Ga}$ -DOTATATE PET/CT scan; C, anterior  $^{177}\text{Lu}$ -octreotate scintigram; and D, coronal posttreatment MIP  $^{68}\text{Ga}$ -DOTATATE PET/CT scan are shown. B, E, The axial CT components of the pretreatment, B, and posttreatment, E,  $^{68}\text{Ga}$ -DOTATATE PET/CT examinations also are shown.

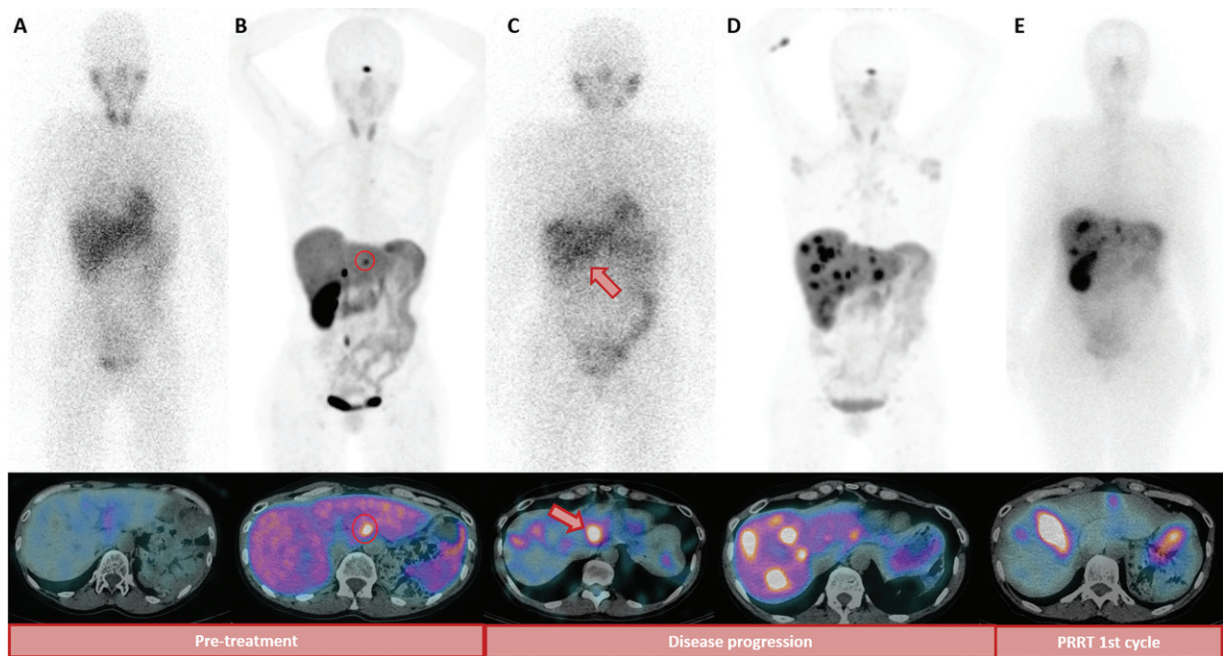


**Figure 25.** Tumor heterogeneity and treatment selection guided by molecular imaging in a 49-year-old patient with metastatic pheochromocytoma. *A*, Anterior  $^{131}\text{I}$ -MIBG WBS (top) and axial SPECT/CT (bottom) findings were negative. *B*, Coronal MIP (top) and axial (bottom)  $^{68}\text{Ga}$ -DOTATATE PET/CT images show low-volume liver disease (red circle). *C*, *D*, Two years later, the patient was found to have progressive liver disease, which was of low volume (arrows in *C*) at anterior  $^{131}\text{I}$ -MIBG WBS (top) and axial (bottom)  $^{68}\text{Ga}$ -DOTATATE MIP PET/CT, *C*, and of high volume at coronal MIP (top) and axial (bottom)  $^{68}\text{Ga}$ -DOTATATE PET/CT, *D*. These findings guided the selection of PRRT treatment. *E*, Posttherapeutic anterior  $^{177}\text{Lu}$ -DOTATATE WBS (top) and axial SPECT/CT (bottom) scans show effective delivery of the therapeutic radionuclide to the target lesions.

use radionuclides with increasing energies and less penetrability. Using dosimetric approaches may help to predict the toxicity from irradiation of nontarget areas.

Response assessment is another area of limitation, as there is no clear and sufficiently studied criteria for response assessment with use of some of the modern theranostic imaging techniques such as  $^{68}\text{Ga}$ -PSMA and  $^{68}\text{Ga}$ -DOTATATE PET/CT. This issue is discussed further in the following section. Finally, given the complexity of many theranostic approaches, issues involving technology availability, regulatory approval, and financial sustainability also are potential limitations that must be overcome.

### Perspectives

Despite the notable advances and growing volume of research in the field of theranostics in recent years, there are still topics requiring consensus and questions that remain unanswered. Perhaps the biggest question that needs to be answered is how to evaluate treatment response and define progressive disease (Fig 25). There are opinions for and against the use of functional versus conventional anatomic imaging (PET vs CT or MRI) to define progressive disease. The question of which criteria should be used for treatment response assessment requires discussion of the utility of criteria such as the World

Health Organization criteria, Response Evaluation Criteria in Solid Tumors (RECIST), and Positron Emission Tomography Response Criteria in Solid Tumors (PERCIST) and prompts debate regarding new and more reliable response evaluation criteria.

Anatomic imaging has been broadly used for treatment response assessment for decades, with adherence to standards from entities such as the World Health Organization, RECIST, and RECIST 1.1. Nonetheless, the predictable shortcomings of this approach were spotlighted after the advent of hybrid, molecular, and multimodal imaging techniques. Many cancers may exhibit minimal changes in tumor size despite effective or ineffective treatments. Long-term clinical experience and published studies (85) indicate that responses to treatment can manifest not only as reductions in tumor burden due to decreased lesion size but in many cases even as stable disease on interval scans. The stability may result from the replacement of tumoral volume by fibrotic tissue, and conventional imaging may not depict a response when no volume changes are noted (85). For this reason, quantitative and qualitative approaches have been developed by using metabolic assessment with PET.

PERCIST 1.1 established a starting point for use of PET-based response assessment criteria in clinical trials and structured quantitative

clinical reporting. To assess the increase or decrease in the metabolism of different lesions and ultimately the presence and absence of tumor viability, statistically significant changes in the tumor standardized uptake value are considered. The more successful the therapy, the greater the decrease in metabolism intensity. This approach, as compared with conventional imaging alone, has refined treatment response assessment. However, again, limitations in clinical practice have been identified over time.

There is still some uncertainty regarding the assessment of mixed patterns of response, and one of the main caveats is that the enforceability of PERCIST 1.1 applies primarily to FDG scanning. Thus, more careful analysis should be considered when evaluating response with use of other radiotracers, and further studies are required to validate the use of PET with several different non-FDG radiotracers in this scenario (86).

More recently, radiomics and quantitative PET techniques have rapidly gained ground, offering the possibility for more refined parameters to assess tumor heterogeneity and phenotypes and the quantification of total tumor burden. Indexes such as metabolic tumor volume with FDG and molecular imaging tumor volume with other radiotracers have flourished and are believed to facilitate more accurate prognosis estimation and response evaluation. Developments in informatics, algorithms, and automation in recent years have provided hope and opportunities to establish PET as an important prognostic biomarker for many diseases (87,88).

Another unaddressed issue is the use of FDG PET scans in the setting of well-differentiated neoplasms. There is not extensive knowledge and consensus regarding the standardized use of FDG PET for neuroendocrine tumors and prostate cancer in terms of which patients should undergo scanning and in which specific scenarios. Also, current data do not indicate whether FDG positivity alone or tumor burden can have a decisive role in prognosis and survival. Dual radiotracer characterization is generally recommended in cases of SSTR PET-negative lesions and undifferentiated tumors with a Ki-67 index greater than 10%, but there is debate as to whether all patients with metastatic disease can benefit from FDG PET (82,89).

In the setting of prostate cancer, there are similar uncertainties regarding response assessment and progressive disease determination, including diverse opinions regarding whole-body quantification of total tumor burden with FDG and PSMA PET and their clinical effect. However, foremost is the need to establish appropriate well-defined criteria for the indication of FDG PET scans in cases

of prostate cancer, as there is currently no consensus regarding all indications that require further investigation in future studies (62,90,91).

## Recently Introduced Agents

It is not within the scope of this overview article to describe all of the potential theranostic radiopharmaceuticals in detail. With the incorporation of theranostic approaches into clinical practice, progressive radiopharmaceuticals have already been developed with use of the theranostic approach, and initial results show promise. Molecules such as CXCR4 ligands, glucagon-like peptides, and fibroblast activation protein ligands can access many pathways in many cancers, including multiple myeloma, insulinoma, and pancreatic cancer (92,93).

## Combining Theranostics with Other Diagnostic and Treatment Modalities

As mentioned, the more recently developed theranostic procedures have a multidisciplinary foundation. In this sense, integration with other diagnostic modalities and procedures such as genetic testing and liquid biopsy, and even combining theranostic approaches with chemotherapy, external-beam radiation therapy, and immunotherapy seem natural, and it is probably only a matter of time before these combination applications become reality (23,94). Many trials involving theranostics have been designed and described in published works. Examples of the more relevant trials are summarized in Table 4.

## Dosimetry

Radionuclide therapies and external-beam radiation therapy are different therapeutic modalities that share the same basic principle: the delivery of cytotoxic radiation to target tissues with no, or at least tolerable, damage to healthy tissues. The dose of radiation energy absorbed by a determined tissue (measured in grays [joules per kilogram in the International System]) is one of the main parameters that determines the biologic effect (eg, cell death) of radiation. Therefore, the estimation of absorbed radiation (ie, dosimetry) serves as an essential tool for making radiation-based treatments less toxic and more effective. Dosimetry is a well-established approach for routine treatment planning in radiation therapy, since the duration and intensity of irradiation, the region to be irradiated, and the target volume are parameters with relative ease of handling.

On the other hand, the physical and pharmacokinetic interactions of radiopharmaceuticals on a whole-body scale add complexity to the internal dosimetric process required for radionuclide treatments. This makes it technically challenging

**Table 4: Ongoing Clinical Trials Involving Theranostics in Nuclear Medicine**

Disease	Theranostic Approach or Agents	Trial*	Key Intervention(s)	Trial Reference(s)
Neuroendocrine tumors	$^{68}\text{Ga}$ -DOTATATE, $^{177}\text{Lu}$ -DOTATATE, $^{177}\text{Lu}$ -edotreotide	COMPETE	Everolimus vs $^{177}\text{Lu}$ -edotreotide	<i>ClinicalTrials.gov</i> , identifier NCT03049189
		NETTER-2	$^{177}\text{Lu}$ -DOTATATE vs long-acting octreotide in high doses	<i>ClinicalTrials.gov</i> , identifier NCT03972488
		CONTROL NETs	Chemotherapy and radiopeptide treatment combination vs standard therapy alone	<i>ClinicalTrials.gov</i> , identifier NCT02358356
Prostate cancer	$^{68}\text{Ga}$ -PSMA, $^{177}\text{Lu}$ -PSMA	VISION	$^{177}\text{Lu}$ -PSMA vs best supportive care	<i>ClinicalTrials.gov</i> , identifier NCT03511664

\*Expansions of listed trial abbreviations can be found at *ClinicalTrials.gov*.

to translate these measurements from a research environment to routine treatments, which usually are planned on the basis of the total amount of administered radiation (activity) rather than the site-specific absorbed radiation doses (95). Dosimetric techniques in nuclear medicine classically have been focused on establishing the maximal individual tolerated doses of radionuclide, and there are a multitude of studies (96–98) in which the pharmacokinetic properties and biodistribution of classic and recently developed agents have been assessed. This approach has been applied more within a research context and has served as a reference to guide more simple and widely adopted clinical activity-based protocols, as it enables estimation of the highest activities that may be applied to a patient without surpassing radiation limits to critical organs such as the kidneys (~40 Gy, commonly used in patients without risk factors for renal toxicity) and bone marrow (widely used limit, 2 Gy).

Improvements in imaging technology (highlighting hybrid imaging) and dosimetry software, as well as the emergence of recently developed diagnostic radiopharmaceuticals, have enabled better definition of target volumes and their integration with pharmacokinetic and irradiation data, increasing the accuracy of dosimetry, especially in lesion or target dosimetry. Lesion- or organ-based dosimetry approaches can yield parameters that have been extensively studied, such as lesion dose-response correlation, dose-volume histogram, and dose heterogeneity map findings. These capabilities have led to dosimetric data becoming more suitable for correlation with biologic effect and clinical outcomes (99). Further studies and some technical simplification are awaited so that internal dosimetry can assume a central role in routine theranostic planning (100).

## Conclusion

There has been a long path to the incorporation of nuclear medicine into theranostics during the past decades, since Saul Hertz performed the first radioiodine therapy in 1941. The development and progress in this field demonstrate the benefits of personalized medicine. The field of theranostics is part of a breakthrough era in which molecular biology, immunology, immunotherapy, genomics, pharmacogenomics, metabolomics, radiomics, artificial intelligence, and other increasingly refined fields are thriving. Thus, there will probably be less and less demand for mass-produced generalized diagnostic methods and treatments that neglect the intricate biologic peculiarities of each individual, cancer, and histologic subtype.

There is increasing understanding of the extensive cancer heterogeneity between different individuals and even among different cell populations in the same patient. Theranostic approaches are connecting imaging to therapy more than ever, and imaging physicians engaged in this field are being driven to re-exercise their clinical roles. Many lessons have been learned from the developments in this area, and they may be the groundwork for developing new technologies. For this to occur, partnerships between academia and industry should become stronger and more frequent, and regulatory authorities must reduce barriers and keep pace with rapid changes in the field to help convert scientific advances into practical clinical applications. More than a novel approach, the field of theranostics is approaching Paul Ehrlich's originally proposed magic bullet, capable of bringing hope and having a profound effect on the lives of millions of patients.

## References

1. Valent P, Groner B, Schumacher U, et al. Paul Ehrlich (1854–1915) and His Contributions to the Foundation

- and Birth of Translational Medicine. *J Innate Immun* 2016;8(2):111–120.
2. Strebhardt K, Ullrich A. Paul Ehrlich's magic bullet concept: 100 years of progress. *Nat Rev Cancer* 2008;8(6):473–480.
  3. Hricak H. Oncologic imaging: a guiding hand of personalized cancer care. *Radiology* 2011;259(3):633–640.
  4. Jadvar H, Chen X, Cai W, Mahmood U. Radiotheranostics in Cancer Diagnosis and Management. *Radiology* 2018;286(2):388–400.
  5. Funkhouser J. Reinventing pharma: the theranostic revolution. *Curr Drug Discov* 2002;(AUG.):17–19.
  6. DeNardo GL, DeNardo SJ. Concepts, consequences, and implications of theranosis. *Semin Nucl Med* 2012;42(3):147–150.
  7. European Society of Radiology. Medical imaging in personalised medicine: a white paper of the research committee of the European Society of Radiology (ESR). *Insights Imaging* 2015;6(2):141–155.
  8. Hevesy G. The Absorption and Translocation of Lead by Plants: A Contribution to the Application of the Method of Radioactive Indicators in the Investigation of the Change of Substance in Plants. In: Leicester HM, ed. *A Source Book in Chemistry 1900–1950*. Cambridge, Mass: Harvard University Press; 2014.
  9. Silberstein EB. Radioiodine: the classic theranostic agent. *Semin Nucl Med* 2012;42(3):164–170.
  10. Hertz B. Dr. Saul Hertz Discovers the Medical Uses of Radioactive Iodine. In: Ahmadzadehfar H, ed. *Thyroid Cancer: Advances in Diagnosis and Therapy*. London, England: Intech Open; 2016: 1–14. <http://dx.doi.org/10.5772/64609>.
  11. Silberstein EB, Alavi A, Balon HR, et al. The SNMMI practice guideline for therapy of thyroid disease with  $^{131}\text{I}$  3.0. *J Nucl Med* 2012;53(10):1633–1651.
  12. Yordanova A, Eppard E, Kürpig S, et al. Theranostics in nuclear medicine practice. *OncoTargets Ther* 2017;10:4821–4828.
  13. Kratochwil C, Haberkorn U, Giesel FL. Radionuclide Therapy of Metastatic Prostate Cancer. *Semin Nucl Med* 2019;49(4):313–325.
  14. Intenzo CM, Dam HQ, Manzone TA, Kim SM. Imaging of the thyroid in benign and malignant disease. *Semin Nucl Med* 2012;42(1):49–61.
  15. Haugen BR, Alexander EK, Bible KC, et al. 2015 American Thyroid Association Management Guidelines for Adult Patients with Thyroid Nodules and Differentiated Thyroid Cancer: The American Thyroid Association Guidelines Task Force on Thyroid Nodules and Differentiated Thyroid Cancer. *Thyroid* 2016;26(1):1–133.
  16. Mallick U, Harmer C, Yap B, et al. Ablation with low-dose radioiodine and thyrotropin alfa in thyroid cancer. *N Engl J Med* 2012;366(18):1674–1685.
  17. Schlumberger M, Catargi B, Borget I, et al. Strategies of radioiodine ablation in patients with low-risk thyroid cancer. *N Engl J Med* 2012;366(18):1663–1673.
  18. Drude N, Tienken L, Mottaghy FM. Theranostic and nanotheranostic probes in nuclear medicine. *Methods* 2017;130:14–22.
  19. Sisson JC, Yanik GA. Theranostics: evolution of the radiopharmaceutical meta-iodobenzylguanidine in endocrine tumors. *Semin Nucl Med* 2012;42(3):171–184.
  20. Parisi MT, Eslamy H, Park JR, Shulkin BL, Yanik GA.  $^{131}\text{I}$ -Metaiodobenzylguanidine Theranostics in Neuroblastoma: Historical Perspectives—Practical Applications. *Semin Nucl Med* 2016;46(3):184–202.
  21. Carrasquillo JA, Pandit-Taskar N, Chen CC. I-131 Metaiodobenzylguanidine Therapy of Pheochromocytoma and Paraganglioma. *Semin Nucl Med* 2016;46(3):203–214.
  22. Wilson JS, Gains JE, Moroz V, Wheatley K, Gaze MN. A systematic review of  $^{131}\text{I}$ -meta iodobenzylguanidine molecular radiotherapy for neuroblastoma. *Eur J Cancer* 2014;50(4):801–815.
  23. Modlin IM, Oberg K, Chung DC, et al. Gastroenteropancreatic neuroendocrine tumours. *Lancet Oncol* 2008;9(1):61–72.
  24. Krenning EP, Kwekkeboom DJ, Bakker WH, et al. Somatostatin receptor scintigraphy with [ $^{111}\text{In}$ -DTPA-D-Phe1]- and [ $^{123}\text{I}$ -Tyr3]-octreotide: the Rotterdam experience with more than 1000 patients. *Eur J Nucl Med* 1993;20(8):716–731.
  25. Krenning EP, Bakker WH, Breeman WA, et al. Localisation of endocrine-related tumours with radioiodinated analogue of somatostatin. *Lancet* 1989;1(8632):242–244.
  26. Stoltz B, Weckbecker G, Smith-Jones PM, Albert R, Raulf F, Bruns C. The somatostatin receptor-targeted radiotherapeutic [ $^{90}\text{Y}$ -DOTA-DPhe1, Tyr3]octreotide ( $^{90}\text{Y}$ -SMT 487) eradicates experimental rat pancreatic CA 20948 tumours. *Eur J Nucl Med* 1998;25(7):668–674.
  27. Krenning EP, Kwekkeboom DJ, Valkema R, Pauwels S, Kvols LK, DeJong M. Peptide receptor radionuclide therapy. *Ann N Y Acad Sci* 2004;1014(1):234–245.
  28. Kwekkeboom DJ, Bakker WH, Kam BL, et al. Treatment of patients with gastro-entero-pancreatic (GEP) tumours with the novel radiolabelled somatostatin analogue [ $^{177}\text{Lu}$ -DOTA(0),Tyr3]octreotate. *Eur J Nucl Med Mol Imaging* 2003;30(3):417–422.
  29. Hofmann M, Maecke H, Börner R, et al. Biokinetics and imaging with the somatostatin receptor PET radioligand ( $^{68}\text{Ga}$ -DOTATOC: preliminary data. *Eur J Nucl Med* 2001;28(12):1751–1757.
  30. Singh S, Poon R, Wong R, Metser U.  $^{68}\text{Ga}$  PET Imaging in Patients With Neuroendocrine Tumors: A Systematic Review and Meta-analysis. *Clin Nucl Med* 2018;43(11):802–810.
  31. Levine R, Krenning EP. Clinical history of the theranostic radionuclide approach to neuroendocrine tumors and other types of cancer: historical review based on an interview of Eric P. Krenning by Rachel Levine. *J Nucl Med* 2017;58(suppl 2):3S–9S.
  32. Öberg K, Knigge U, Kwekkeboom D, Perren A; ESMO Guidelines Working Group. Neuroendocrine gastro-entero-pancreatic tumors: ESMO clinical practice guidelines for diagnosis, treatment and follow-up. *Ann Oncol* 2012;23(suppl 7):vii124–vii130.
  33. Shah MH, Goldner WS, Halfdanarson TR, et al. NCCN Guidelines Insights: Neuroendocrine and Adrenal Tumors, Version 2.2018. *J Natl Compr Canc Netw* 2018;16(6):693–702.
  34. Hope TA, Bergsland EK, Bozkurt MF, et al. Appropriate use criteria for somatostatin receptor PET imaging in neuroendocrine tumors. *J Nucl Med* 2018;59(1):66–74.
  35. Bodei L, Mueller-Brand J, Baum RP, et al. The joint IAEA, EANM, and SNMMI practical guidance on peptide receptor radionuclide therapy (PRRNT) in neuroendocrine tumours. *Eur J Nucl Med Mol Imaging* 2013;40(5):800–816.
  36. Rindi G. The ENETS guidelines: the new TNM classification system. *Tumori* 2010;96(5):806–809.
  37. Mitra ES. Neuroendocrine Tumor Therapy:  $^{177}\text{Lu}$ -DOTATATE. *AJR Am J Roentgenol* 2018;211(2):278–285.
  38. Demirci E, Kabasakal L, Toklu T, et al.  $^{177}\text{Lu}$ -DOTATATE therapy in patients with neuroendocrine tumours including high-grade (WHO G3) neuroendocrine tumours: response to treatment and long-term survival update. *Nucl Med Commun* 2018;39(8):789–796.
  39. Taïeb D, Jha A, Treglia G, Pacak K. Molecular imaging and radionuclide therapy of pheochromocytoma and paraganglioma in the era of genomic characterization of disease subgroups. *Endocr Relat Cancer* 2019;26(11):R627–R652.
  40. Kong G, Grozinsky-Glasberg S, Hofman MS, et al. Efficacy of peptide receptor radionuclide therapy for functional metastatic paraganglioma and pheochromocytoma. *J Clin Endocrinol Metab* 2017;102(9):3278–3287.
  41. Mercado-Asis LB, Wolf KI, Jochmanova I, Taïeb D. Pheochromocytoma: a genetic and diagnostic update. *Endocr Pract* 2018;24(1):78–90.
  42. Gains JE, Bomanji JB, Fersht NL, et al.  $^{177}\text{Lu}$ -DOTATATE molecular radiotherapy for childhood neuroblastoma. *J Nucl Med* 2011;52(7):1041–1047.
  43. Iten F, Müller B, Schindler C, et al. Response to [ $^{90}\text{Y}$ -Tritium-DOTA]-TOC treatment is associated with long-term survival benefit in metastasized medullary thyroid cancer: a phase II clinical trial. *Clin Cancer Res* 2007;13(22 Pt 1):6696–6707.
  44. Bartolomei M, Bodei L, De Cicco C, et al. Peptide receptor radionuclide therapy with ( $^{90}\text{Y}$ -DOTATOC in

- recurrent meningioma. *Eur J Nucl Med Mol Imaging* 2009;36(9):1407–1416.
45. Strosberg J, El-Haddad G, Wolin E, et al. Phase 3 trial of 177Lu-dotatate for midgut neuroendocrine tumors. *N Engl J Med* 2017;376(2):125–135.
  46. Strosberg J, Wolin E, Chasen B, et al. Health-Related Quality of Life in Patients With Progressive Midgut Neuroendocrine Tumors Treated With 177Lu-Dotatate in the Phase III NETTER-1 Trial. *J Clin Oncol* 2018;36(25):2578–2584.
  47. Cremonesi M, Ferrari M, Bodei L, Tosi G, Paganelli G. Dosimetry in peptide radionuclide receptor therapy: a review. *J Nucl Med* 2006;47(9):1467–1475.
  48. Forrer F, Krenning EP, Kooij PP, et al. Bone marrow dosimetry in peptide receptor radionuclide therapy with [177Lu-DOTA(0),Tyr(3)]octreotate. *Eur J Nucl Med Mol Imaging* 2009;36(7):1138–1146.
  49. Cremonesi M, Botta F, Di Dia A, et al. Dosimetry for treatment with radiolabelled somatostatin analogues: a review. *Q J Nucl Med Mol Imaging* 2010;54(1):37–51.
  50. American Cancer Society. *Cancer Facts & Figures* 2017. Atlanta, Ga: American Cancer Society, 2017.
  51. Barbosa FG, Queiroz MA, Nunes RF, et al. Revisiting Prostate Cancer Recurrence with PSMA PET: Atlas of Typical and Atypical Patterns of Spread. *RadioGraphics* 2019;39(1):186–212.
  52. Scher HI, Fizazi K, Saad F, et al. Increased survival with enzalutamide in prostate cancer after chemotherapy. *N Engl J Med* 2012;367(13):1187–1197.
  53. Kratochwil C, Giesel FL, Eder M, et al. [177Lu]Lutetium-labelled PSMA ligand-induced remission in a patient with metastatic prostate cancer. *Eur J Nucl Med Mol Imaging* 2015;42(6):987–988.
  54. Afshar-Oromieh A, Avtzi E, Giesel FL, et al. The diagnostic value of PET/CT imaging with the (68)Ga-labelled PSMA ligand HBED-CC in the diagnosis of recurrent prostate cancer. *Eur J Nucl Med Mol Imaging* 2015;42(2):197–209.
  55. Hofman MS, Hicks RJ, Maurer T, Eiber M. Prostate-specific membrane antigen PET: clinical utility in prostate cancer, normal patterns, pearls, and pitfalls. *RadioGraphics* 2018;38(1):200–217.
  56. Eiber M, Maurer T, Souvatzoglou M, et al. Evaluation of Hybrid 68Ga-PSMA Ligand PET/CT in 248 Patients with Biochemical Recurrence After Radical Prostatectomy. *J Nucl Med* 2015;56(5):668–674.
  57. Rauscher I, Maurer T, Fendler WP, Sommer WH, Schwaiger M, Eiber M. (68)Ga-PSMA ligand PET/CT in patients with prostate cancer: how we review and report. *Cancer Imaging* 2016;16(1):14.
  58. Ballas LK, de Castro Abreu AL, Quinn DI. What Medical, Urologic, and Radiation Oncologists Want from Molecular Imaging of Prostate Cancer. *J Nucl Med* 2016;57(suppl 3):S6–S12S.
  59. Fendler WP, Rahbar K, Herrmann K, Kratochwil C, Eiber M. 177Lu-PSMA radioligand therapy for prostate cancer. *J Nucl Med* 2017;58(8):1196–1200.
  60. Emmett L, Willowson K, Violet J, Shin J, Blanksby A, Lee J. Lutetium 177 PSMA radionuclide therapy for men with prostate cancer: a review of the current literature and discussion of practical aspects of therapy. *J Med Radiat Sci* 2017;64(1):52–60.
  61. Yong KJ, Milenic DE, Baidoo KE, Brechbiel MW. Mechanisms of Cell Killing Response from Low Linear Energy Transfer (LET) Radiation Originating from (177)Lu Radioimmunotherapy Targeting Disseminated Intraperitoneal Tumor Xenografts. *Int J Mol Sci* 2016;17(5):E736.
  62. Hofman MS, Violet J, Hicks RJ, et al. [177Lu]-PSMA-617 radionuclide treatment in patients with metastatic castration-resistant prostate cancer (LuPSMA trial): a single-centre, single-arm, phase 2 study. *Lancet Oncol* 2018;19(6):825–833.
  63. Calopedos RJS, Chalasani V, Asher R, Emmett L, Woo HH. Lutetium-177-labelled anti-prostate-specific membrane antigen antibody and ligands for the treatment of metastatic castrate-resistant prostate cancer: a systematic review and meta-analysis. *Prostate Cancer Prostatic Dis* 2017;20(3):352–360.
  64. Rahbar K, Ahmadzadehfar H, Kratochwil C, et al. German multicenter study investigating 177Lu-PSMA-617 radioligand therapy in advanced prostate cancer patients. *J Nucl Med* 2017;58(1):85–90.
  65. Ahmadzadehfar H, Wegen S, Yordanova A, et al. Overall survival and response pattern of castration-resistant metastatic prostate cancer to multiple cycles of radioligand therapy using [177Lu]Lu-PSMA-617. *Eur J Nucl Med Mol Imaging* 2017;44(9):1448–1454.
  66. Kratochwil C, Giesel FL, Stefanova M, et al. PSMA-targeted radionuclide therapy of metastatic castration-resistant prostate cancer with 177Lu-Labeled PSMA-617. *J Nucl Med* 2016;57(8):1170–1176.
  67. Rahbar K, Bode A, Weckesser M, et al. Radioligand therapy with 177Lu-PSMA-617 as a novel therapeutic option in patients with metastatic castration resistant prostate cancer. *Clin Nucl Med* 2016;41(7):522–528.
  68. Parker C, Nilsson S, Heinrich D, et al. Alpha emitter radium-223 and survival in metastatic prostate cancer. *N Engl J Med* 2013;369(3):213–223.
  69. Du Y, Carrio I, De Vincentis G, et al. Practical recommendations for radium-223 treatment of metastatic castration-resistant prostate cancer. *Eur J Nucl Med Mol Imaging* 2017;44(10):1671–1678.
  70. Parker CC, Coleman RE, Sartor O, et al. Three-year Safety of Radium-223 Dichloride in Patients with Castration-resistant Prostate Cancer and Symptomatic Bone Metastases from Phase 3 Randomized Alpharadin in Symptomatic Prostate Cancer Trial. *Eur Urol* 2018;73(3):427–435.
  71. Heinrich D, Bektic J, Bergman AM, et al. The Contemporary Use of Radium-223 in Metastatic Castration-resistant Prostate Cancer. *Clin Genitourin Cancer* 2017. 10.1016/j.clgc.2017.08.020. Published online September 6, 2017.
  72. Eckert F, Gaip US, Niedermann G, et al. Beyond checkpoint inhibition: immunotherapeutic strategies in combination with radiation. *Clin Transl Radiat Oncol* 2017;2:29–35.
  73. Murthy R, Nunez R, Szklaruk J, et al. Yttrium-90 microsphere therapy for hepatic malignancy: devices, indications, technical considerations, and potential complications. *RadioGraphics* 2005;25(suppl 1):S41–S55.
  74. Sangro B, Inarrairaegui M, Bilbao JI. Radioembolization for hepatocellular carcinoma. *J Hepatol* 2012;56(2):464–473.
  75. Kostakoglu L, Agress H Jr, Goldsmith SJ. Clinical role of FDG PET in evaluation of cancer patients. *RadioGraphics* 2003;23(2):315–340; quiz 533.
  76. James OG, Christensen JD, Wong TZ, Borges-Neto S, Kowek LM. Utility of FDG PET/CT in inflammatory cardiovascular disease. *RadioGraphics* 2011;31(5):1271–1286.
  77. Brown RKJ, Bohnen NI, Wong KK, Minoshima S, Frey KA. Brain PET in suspected dementia: patterns of altered FDG metabolism. *RadioGraphics* 2014;34(3):684–701.
  78. Lardinois D, Weder W, Hany TF, et al. Staging of non-small-cell lung cancer with integrated positron-emission tomography and computed tomography. *N Engl J Med* 2003;348(25):2500–2507.
  79. Munkley J, Elliott DJ. Hallmarks of glycosylation in cancer. *Oncotarget* 2016;7(23):35478–35489.
  80. Warburg O. On the origin of cancer cells. *Science* 1956;123(3191):309–314.
  81. Bahri H, Laurence L, Edeline J, et al. High prognostic value of 18F-FDG PET for metastatic gastroenteropancreatic neuroendocrine tumors: a long-term evaluation. *J Nucl Med* 2014;55(11):1786–1790.
  82. Niederle B, Pape UF, Costa F, et al. ENETS consensus guidelines update for neuroendocrine neoplasms of the jejunum and ileum. *Neuroendocrinology* 2016;103(2):125–138.
  83. Chan DLH, Pavlakis N, Schembri GP, et al. Dual somatostatin receptor/FDG PET/CT imaging in metastatic neuroendocrine tumours: proposal for a novel grading scheme with prognostic significance. *Theranostics* 2017;7(5):1149–1158.
  84. Ulaner GA, Hyman DM, Lyashchenko SK, Lewis JS, Carrasquillo JA. <sup>89</sup>Zr-trastuzumab PET/CT for detection of human epidermal growth factor receptor 2-positive metastases in patients with human epidermal growth factor receptor 2-negative primary breast cancer. *Clin Nucl Med* 2017;42(12):912–917.
  85. van Vliet EI, Krenning EP, Teunissen JJ, Bergsma H, Kam BL, Kwekkeboom DJ. Comparison of response evaluation in patients with gastroenteropancreatic and

- thoracic neuroendocrine tumors after treatment with [177Lu-DOTA0,Tyr3]octreotate. *J Nucl Med* 2013;54(10):1689–1696.
86. Wahl RL, Jacene H, Kasamon Y, Lodge MA. From RECIST to PERCIST: evolving considerations for PET response criteria in solid tumors. *J Nucl Med* 2009;50(suppl 1):122S–150S.
87. Schöder H, Moskowitz C. Metabolic tumor volume in lymphoma: hype or hope? *J Clin Oncol* 2016;34(30):3591–3594.
88. Winther-Larsen A, Fledelius J, Sorensen BS, Meldgaard P. Metabolic tumor burden as marker of outcome in advanced EGFR wild-type NSCLC patients treated with erlotinib. *Lung Cancer* 2016;94:81–87.
89. Sansovini M, Severi S, Ianniello A, et al. Long-term follow-up and role of FDG PET in advanced pancreatic neuroendocrine patients treated with 177Lu-DOTATATE. *Eur J Nucl Med Mol Imaging* 2017;44(3):490–499. [Published correction appears in Eur J Nucl Med Mol Imaging 2017;44(2):352.]
90. Suman S, Parghane RV, Joshi A, et al. Therapeutic efficacy, prognostic variables and clinical outcome of 177Lu-PSMA-617 PRRT in progressive mCRPC following multiple lines of treatment: prognostic implications of high FDG uptake on dual tracer PET-CT vis-à-vis Gleason score in such cohort. *Br J Radiol* 2019;92(1104):20190380.
91. Perez PM, Hope TA, Behr SC, van Zante A, Small EJ, Flavell RR. Intertumoral Heterogeneity of 18F-FDG and 68Ga-PSMA Uptake in Prostate Cancer Pulmonary Metastases. *Clin Nucl Med* 2019;44(1):e28–e32.
92. Walenkamp AME, Lapa C, Herrmann K, Wester HJ. CXCR4 ligands: the next big hit? *J Nucl Med* 2017;58(suppl 2):77S–82S.
93. Watabe T, Liu Y, Kaneda-Nakashima K, et al. Theranostics Targeting Fibroblast Activation Protein in the Tumor Stroma: 64Cu- and 225Ac-Labeled FAPI-04 in Pancreatic Cancer Xenograft Mouse Models. *J Nucl Med* 2020;61(4):563–569.
94. Virgolini I, Innsbruck Team. Peptide receptor radionuclide therapy (PRRT): clinical significance of re-treatment? *Eur J Nucl Med Mol Imaging* 2015;42(13):1949–1954.
95. Sapienza MT, Willegaignon J. Radionuclide therapy: current status and prospects for internal dosimetry in individualized therapeutic planning. *Clinics (São Paulo)* 2019;74:e835.
96. Benua RS, Cicale NR, Sonenberg M, Rawson RW. The relation of radioiodine dosimetry to results and complications in the treatment of metastatic thyroid cancer. *Am J Roentgenol Radium Ther Nucl Med* 1962;87:171–182.
97. Kabasakal L, AbuQeitah M, Aygün A, et al. Pre-therapeutic dosimetry of normal organs and tissues of (177)Lu-PSMA-617 prostate-specific membrane antigen (PSMA) inhibitor in patients with castration-resistant prostate cancer. *Eur J Nucl Med Mol Imaging* 2015;42(13):1976–1983.
98. Gupta SK, Singla S, Thakral P, Bal CS. Dosimetric analyses of kidneys, liver, spleen, pituitary gland, and neuroendocrine tumors of patients treated with 177Lu-DOTATATE. *Clin Nucl Med* 2013;38(3):188–194.
99. Sgouros G, Hobbs RF. Dosimetry for radiopharmaceutical therapy. *Semin Nucl Med* 2014;44(3):172–178.
100. Eberlein U, Cremonesi M, Lassmann M. Individualized dosimetry for theranostics: necessary, nice to have, or counterproductive? *J Nucl Med* 2017;58(suppl 2):97S–103S.